INVESTIGATING THE ISOTOPIC COMPOSITION OF REACTIVE NITROGEN IN A SOUTH TEXAS ESTUARY (BAFFIN BAY)

A Thesis

by

JACQUELYN CAMPBELL

BS, Texas A&M University, 2012

Submitted in Partial Fulfillment of the Requirements for the Degree of

MASTER OF SCIENCE

in

COASTAL AND MARINE SYSTEM SCIENCE

Texas A&M University-Corpus Christi
Corpus Christi, Texas

August 2018

August 2018

INVESTIGATING THE ISOTOPIC COMPOSITION OF REACTIVE NITROGEN IN A SOUTH TEXAS ESTUARY (BAFFIN BAY)

A Thesis

by

JACQUELYN CAMPBELL

This thesis meets the standards for scope and quality of
Texas A&M University-Corpus Christi and is hereby approved.

Dr. J.D. Felix
Chairperson

Dr. M. Wetz
Committee Member

Dr. H. Abdulla
Committee Member

August 2018

ABSTRACT

Harmful algal blooms (HABs) have the potential to adversely affect the water quality of estuaries and, consequently, their ability to support healthy and diverse ecosystems. Since 1989, Baffin Bay, a semi-arid south Texas estuary, has experienced harmful algal blooms. This work investigates the stable isotopic composition of reactive nitrogen (Nr) (δ^{15}N-DON, δ^{15}N-NH_4^+, and δ^{15}N-NO_3^-) in samples collected monthly at nine stations over the period of one year and provides insight into Nr sources and processing in Baffin Bay. The following seasonal stages summarize the influences affecting δ^{15}N values throughout the study: 1) Elevated δ^{15}N-DIN values (4.9‰ ± 5‰) in the winter indicate the influence of a source of DIN with a relatively high δ^{15}N such as wastewater or septic effluent, which may also contribute to elevated DON concentrations (46.4 µM ± 10 µM) and δ^{15}N-DON values (9.5‰ ± 2‰). 2) The increase of NH_4^+ concentrations in the spring from run off concurrent with steady δ^{15}N-DIN values (3.6‰ ± 6 ‰) implies phytoplankton assimilation of DON as evidenced by high δ^{15}N-DON values (12‰ ± 6‰) and low DON concentrations (36µM ± 13.2 µM). 3) Evidence of photo-ammonification is observed throughout the summer due to elevated δ^{15}N-DON values (10.5‰ ± 3‰) and low DON concentrations concurrent with low δ^{15}N-DIN (-1‰ ± 5‰) and elevated NH_4^+ concentrations. 4) The accumulation of DON concentrations in the fall are consistent with phytoplankton detritus, which is supported by the decrease in δ^{15}N-DON value averages in the fall and winter (9.8‰ ± 2 ‰). Remineralization during this stage is supported by low δ^{15}N-DIN values (-2.3‰ ± 4.4‰). Additionally, salinity gradients and cross plots of δ^{15}N values and concentrations support the idea that while both mixing and processing can influence δ^{15}N values and patterns observed throughout the year, Nr processing (i.e. photo-ammonification, phytoplankton uptake, bacterial mineralization) may be the dominant mechanism for N cycling in Baffin Bay. Overall, this study

increases constraints on the Nr isotope budget in Baffin Bay and offers insight into the role of DON in the N-cycle in a south Texas estuary.

ACKNOWLEDGEMENTS

I would like to thank my committee chair, Dr. J.D. Felix, and my committee members, Dr. H. Abdulla, Dr. M. Wetz, for their guidance and support throughout the course of this research. I would like to thank Kenneth Hayes for the concentration analysis, as well as University of Pittsburgh, Washington State University, and UC Davis for isotopic analysis. I would also like to thank Sagar Shrestha, Alex Berner, Audrey Douglas, Emily Cira, and all my friends and colleagues who have volunteered their time and provided valuable input and insights for this research. Finally, I want to thank the Geological Society of America (GSA), National Science Foundation, and Coastal Bend Bays and Estuaries Program (CBBEP) for supporting this research was well as the Baffin Bay Water Quality Monitoring Volunteer group for sampling and providing concentration data.

TABLE OF CONTENTS

LIST OF FIGURES

FIGURES PAGE

LIST OF TABLES

TABLES PAGE

CHAPTER I- INTRODUCTION

Nr (reactive nitrogen) inputs from runoff, riverine input, and atmospheric deposition and transport are an important source of Nr to the coastal area (Paerl et al., 2002; Seitzinger at al., 2002; Gardner et al., 2006; Kelly, 2008; Mooney and McClelland, 2012; Paerl et al., 2016). Increases in Nr inputs can dramatically alter these ecosystems and generally stimulates plankton biomass and primary productivity in many marine environments (Kelly, 2008; Seitzinger at al., 2002; Pennock et al., 1999). Most previous studies evaluating Nr loading and the consequences for affected ecosystems have focused primarily on the dissolved inorganic nitrogen (DIN) portion (i.e. nitrite, nitrate, and ammonium) of the total dissolved nitrogen (TDN) pool due to the fact that dissolved organic nitrogen (DON) was historically considered primarily recalcitrant and resistant to biological degradation, and generally unavailable as a nutrient for organisms in marine environments (Seitzinger at al., 2002; Berman and Bronk, 2003). However, more recent studies have shown that DON is a dynamic participant in the N cycle. Alkhatib et al., 2012 illustrated that while the average oceanic DON pool may consist of refractory DON, it cannot be discounted that a considerable portion of this DON fluxes out of the marine sediment and must contribute to the oceanic DIN pool. Otherwise, it would be difficult to rationalize the contrast between the large DON concentrations contributed to by coastal benthic fluxes, and the low ambient oceanic DON concentration (Alkhatib et al., 2012). Dissolved organic nitrogen (DON) can constitute a large portion (10% to 80%) of the total dissolved nitrogen (TDN) pool in coastal ecosystems, which could potentially play an active role in the N-cycle in estuarine and coastal ecosystems (Schlarbaum et al., 2010; Seitzinger et al., 2002). A study conducted on rainwater collected in Philadelphia, Pennsylvania concluded that approximately 45–75% of the DON in the atmospheric deposition was biologically available and rapidly utilized by microorganisms (Seitzinger and

Sanders, 1999). Thibodeau et al., 2017 suggests DON from riverine input can contribute up to six times the amount of nitrogen than that of riverine nitrate, and approximately 62 to 76% of the released DON is removed within shelf waters, indicating lability and influence on primary productivity. Another study in New Jersey concluded that runoff from anthropogenic inputs such as urban/suburban runoff have higher proportions of bioavailable DON (59% ± 11), than agricultural pasture sites (30% ± 14), and forested land (23% ± 19) (Seitzinger et al., 2002). Collective data from bioassays suggest that the bioavailable portion of the DON pool can be consumed within estuaries that have residence times ranging from weeks to months, and where residence times are shorter, the DON will serve as a source of N to coastal waters (Bronk et al., 2007). This source of biologically available DON can play an important role in assimilatory and dissimilatory biological processes in coastal waters. It has been evidenced in coastal systems that lower levels of DIN to DON in a system caused by external factors (i.e. drought conditions which limit the amount of riverine input and consequently the amount of IN loaded) can be favorable for dinoflagellates and cyanobacteria, which can cause the establishment of harmful algal blooms (Bronk et al., 2007; Schlarbaum et al., 2010).

Baffin Bay, a unique south Texas ecosystem that is a significant contributor to the regional economy due to revenue generated from its tourism and fishing industry, has been adversely affected by harmful algal blooms (HABs) since 1989. These blooms are dependent on forms of reactive (or bioavailable) nitrogen (Nr) (i.e. nitrite (NO_2^-), ammonium (NH_4^+), dissolved organic nitrogen (DON)) as nutrients to survive. The primary species of HAB native to the Baffin Bay region, *Aureoumbra lagunensis* (collectively known as brown tide), is unable to utilize NO_3^- as a nutrient source, but instead relies on certain forms of reduced nitrogen (such as DON and NH_4^+) for survival (DeYoe and Suttle, 1994). DON levels in Baffin Bay (77 ± 10 μM) exceed the DON

concentrations of not only typical Texas estuaries, but estuaries worldwide (Wetz et al., 2017; Sipler and Bronk, 2015). Additionally, DON accounts for ~90% of the total dissolved nitrogen (TDN) in Baffin Bay, followed by NH_4^+ at ~8%, and NO_3^-+NO_2^- contributing ~2% (Wetz, unpublished data) [Figure 1].

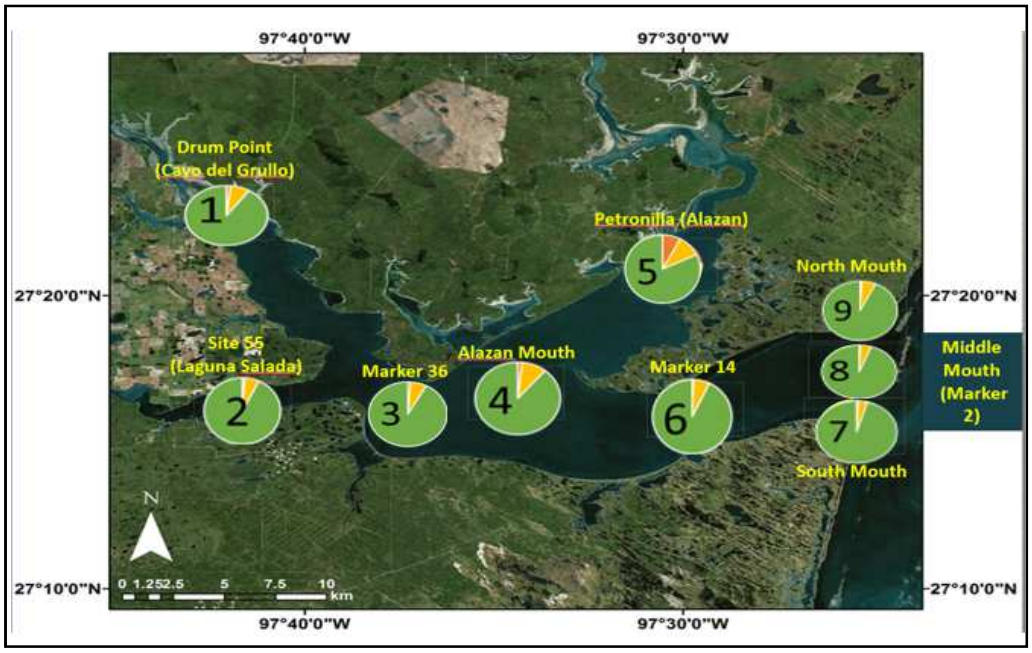

Figure 1. Baffin Bay water sampling sites marked by site number and pie chart. Pie charts represent the nitrogen concentration contribution of dissolved organic nitrogen (green), ammonium (yellow) and nitrite + nitrate (red) for each site. (Wetz, unpublished data).

The distinctive ability of brown tide to utilize dissolved organic nitrogen (DON) as a nutrient allows the bloom to establish where competing organisms reliant on dissolved inorganic nitrogen (DIN) are unable to persist (DeYoe and Suttle, 1994; Mulholland et al., 2004, Bronk et al., 2007; Schlarbaum et al., 2010). An example of this occurred with a different species of brown tide (*Aureococcus anophagefferens*) in the Great South Bay (GSB), New York at a time when the

concentrations of DON were elevated, and the DIN concentrations were low (Gobler et al., 2002). The ecological impacts of *A. lagunensis* blooms include decreased abundance of sea grass beds and essential habitat for organisms (i.e. juvenile shrimp, crabs, and fish) as well as diminished biomass and diversity of benthic invertebrates due primarily to light attenuation (Bricelj and Lonsdale, 1997; Fry and Parker, 1979). The proliferation of brown tide can also have adverse economic consequences. A 1985 brown tide event in Peconic Bay in New York resulted in the elimination of a significant bay scallop fishery, which, despite restoration efforts, could not be reestablished. Not only did this affect the biodiversity of the estuary's ecosystem, it resulted in the loss of an estimated 3-million-dollar surplus annually due to the absence of this scallop fishery (Hogland and Scatasta, 2006). The mitigation of *A. lagunensis* blooms, and, in turn, avoidance of the negative ecological and economic impacts associated with their colonization, is contingent on understanding the physical, ecological, and nutritional conditions under which these organisms can thrive. Due to the dependence of *A. lagunensis* on certain reduced forms of nitrogen as an energy source and the elevated concentrations of DON throughout the Baffin Bay, it is important to identify the origin of this Nr as well as how it is being processed as it cycles through the ecosystem.

A method of identifying sources and understanding the processing of Nr in the environment is to analyze its stable isotopic composition. Isotope analysis has been used in many studies to trace sources of nitrogen in a variety of systems because sources often have a distinct isotope ratio (Heaton, 1986). These unique ratios of ^{15}N:^{14}N act as a fingerprint for different nutrient sources and processing mechanisms. This approach has been used extensively to investigate inorganic nitrogen (NO_3^-, NO_2^-, NH_4^+) processing in estuaries, bays, oceans and rivers (Burns et al., 2009; Wankel et al., 2009, Knapp et al., 2005; Alkhatib et al., 2012) and recent advances in isotope

instrumentation and analysis methods have allowed for isotopic studies investigating DON **(**Tsunogai et al., 2008**).** Characterizing the dominant nitrogen processes in Baffin Bay by determining the isotopic composition of Nr can be used for a better understanding of how organisms (specifically HABs) are processing Nr (specifically DON). This information can be useful and applicable to estuarine ecosystems in various settings, advancing scientific progress towards mitigating blooms. Bloom mitigation could eventually improve the health of impacted ecosystems, which will in turn affect the quality of the ecosystem services it can provide to the communities that depend on them.

In order to understand the potential processing pathways of Nr in Baffin Bay and how they affect the isotopic composition of Nr species, it is important to identify potential sources of Nr and know their characteristic $\delta^{15}N$ signatures. Nr in estuarine environments have both autochthonous and allochthonous sources. Allochthonous, anthropogenic sources of Nr include fertilizers, municipal sewage, animal waste, and atmospheric deposition (Kendall et al., 2007). Some autochthonous forms of Nr (DON specifically) can be released by the process of viral lysis or cell death of bacteria, phytoplankton, and macrophytes, as well as grazing and excretion by zooplankton (Berman and Bronk, 2003). Each source of Nr has a characteristic isotopic signature; for example: ammonium and nitrate from wet deposition ($\delta^{15}N$~-15 to +15‰), nitrate in inorganic fertilizers ($\delta^{15}N$~ -8 to +7‰), manure and septic waste ($\delta^{15}N$~ +2 to +25‰), marine organisms ($\delta^{15}N$ values of ~0 to +22‰). (Kendall et. al, 2007; Heaton, 1986) [See Table 1]**.** Additionally, each processing mechanism for various forms of Nr will have individual fractionation effects such as biological nitrogen fixation (-2.02 ± 2.02‰ (median -2.2‰)), mineralization (-2.33 to -1.43‰), nitrification (-29.6 ±4.9‰ (median -27.2‰)), denitrification (-38 ± -2.6‰ (mean: -17.8 ± 10.3‰)) (Denk et al., 2017 and references therein) [See Table 2]. Using these known isotopic source values,

as well as the isotopic fractionation effects for known processes, previous studies have been able to elucidate the dominant processes and sources of nitrogen in various aquatic systems (Knapp, et al., 2005, Hadas et al., 2009, and Schlarbaum et al., 2010, Thibodeau et al., 2017).

NO_3^- Source $\delta^{15}N$ Values	$\delta^{15}N$ Values	Source
Wastewater/Septic Effluent	+10 to + 25‰	Kendall et al., 2007
Synthetic Fertilizer	−5 to + 8‰	Umezawa et al., 2008
Animal Manure	+10 to + 22‰	Bateman et al., 2005
Wet Deposition	−15 to + 15‰	Kendall et al., 2007
NH_4^+ Source $\delta^{15}N$ Values	$\delta^{15}N$ Values	Source
Untreated Sewage	+5 to + 9‰	Cole et al., 2006
Synthetic Fertilizers	-2 to +2 ‰	Choi et al., 2017
Wet Deposition	-15 to 15 ‰	Kendall et al., 2007
Organic Nitrogen Source $\delta^{15}N$ Values	$\delta^{15}N$ Values	Source
Synthetic Fertilizer (Urea)	~-6 to +2‰	Choi et al., 2017
Organic Fertilizers	~-3.9 to +37‰	Bateman & Kelly, 2007
Wet Deposition	-7.9 to +3.8‰	Lee et al., 2012

Table 1. Table of various sources of $\delta^{15}N$ values from common nitrogen sources.

Process	Enrichment Factor (ε)	Source
Nitrification	+14 to + 38‰	Sigman et al., 2009
Denitrification	+5 to + 30‰	Sigman et al., 2009
DNRA (low oxygen regions)	+20 to + 30‰	Cascotti, 2016
Phytoplankton NO_3^- Uptake	+4 to + 6‰	Cascotti, 2016
NH_4^+ uptake	-9.4 ± 6.6 ‰	Denk et al., 2017
Photo-ammonification	+3 to +10 ‰	Thibodeau et al., 2017
Anammox	~ − 31‰	Brunner et al., 2013
Remineralization	~ ± 1‰	Kendall et al., 2007
N Fixation	−3 to + 1‰	Kendall et al., 2007

Table 2. Table of various enrichment factors associated with nitrogen processing mechanisms.

For example, a study conducted on a lake located in a semi-arid region (Lake Kinneret, Israel), used isotopic compositions of Nr sampled over the course of a year to determine the dominant

seasonal stages of the N cycle of the lake as well as the role of major biological processes (Hadas et al., 2009). The concentration of DON fluctuated significantly throughout the seasons, which suggests lability and an active role in the N-cycling of Lake Kinneret. The δ^{15}N-DON (8 to 11‰) was observed to overlap with the δ^{15}N-POM (particulate organic matter) of Lake Kinneret during late summer and autumn. The δ^{15}N-DON values during these periods suggests phytoplankton blooms from previous seasons as a source of DON.

An alternate study conducted on the turbidity maximum zone (TMZ) of an estuary, which serves as a source of nitrogen to the Elbe estuary, used the isotopic composition of DON+NH_4^+ to determine whether there were any correlations between concentration fluctuations, the processes causing those fluctuations, and whether or not the isotopic signatures during this study had seasonal patterns (Schlarbaum et al., 2010). The study concluded that selective absorption to particles within the TMZ is a sink for DON+NH_4^+ in the estuary and particle-adsorbed DON may be a significant source of DON to the waters in the outer Elbe estuary (Schlarbaum et al., 2010). Additionally, the port of Hamburg was indicated in this study as a clear source of DON and NH_4^+ to the Elbe Estuary due to the relatively elevated concentrations and isotope values of DON+NH_4^+ measured within the port. These elevated isotope values are most likely due to inputs from local sewage treatment plants or local biogenic sources (e.g. animal management operations, hydrocarbons in soil from the decay of organic matter) (Schlarbaum et al., 2010).

There have been a number of studies, including the studies mentioned above, investigating the δ^{15}N-TDN and δ^{15}N-DIN of water samples in order to characterize the N cycle in various marine environments, however, due to analytical capabilities and methodological limitations, very few studies have been able to isolate the δ^{15}N-DON from the δ^{15}N-TDN values unless components of the DIN pool have a minimal contribution to TDN and are discounted (Knapp, et al., 2005, Hadas

et al., 2009, and Schlarbaum et al., 2010). This work investigated the sources and processing mechanisms of Nr in Baffin Bay, a semi-arid south Texas estuary, utilizing concentration fluctuations paired with the $\delta^{15}N$ values associated with the respective forms of Nr including the isolated portion of $\delta^{15}N$-DON. The primary objectives of this study were to 1) investigate the stable isotopic composition of reactive nitrogen (Nr) ($\delta^{15}N$-DON, $\delta^{15}N$-NH_4^+, and $\delta^{15}N$-NO_3) in Baffin Bay samples collected monthly at nine stations over the period of one year, and 2) utilize stable isotope techniques to investigate Nr sources and processing in Baffin Bay. Additionally, since the elevated concentrations of DON make Baffin Bay uniquely suited to investigate its sources and processing, this project aids in characterizing the role of a largely unstudied form of Nr, which provides insight and changes perceptions about the role of DON in nitrogen dynamics as a whole. In summary, the data collected in this study contributes to the limited $\delta^{15}N$-DON measurements available in literature, expands on a method used to separate $\delta^{15}N$-DON from $\delta^{15}N$-TDN values, and increases isotopic constraints on the N cycle in Baffin Bay, Texas.

CHAPTER II- METHODS

A. Study Site

Baffin Bay is a shallow (≤ 2 to 3 m depth) south Texas estuary in the north-western portion of the Gulf of Mexico and is an inlet of the larger Laguna Madre system [See Figure 1] (Simms et al., 2010). Baffin Bay differs from most Gulf of Mexico estuaries in that it is separated from the Gulf of Mexico by the barrier island Padre Island (Simms et al., 2010). Additionally, Baffin Bay is isolated from the larger Laguna Madre system due to several shallow reefs located near the mouth of the bay (Simms et al., 2010). Petronila Creek, Los Olmos Creek, and San Fernando Creek are the three creeks that drain into Baffin Bay, however, their freshwater/riverine discharge is ephemeral, and no other major river discharges are received (An and Gardner, 2002; Simms et al., 2010). The precipitation received by Baffin Bay averages between 60 and 80 cm $year^{-1}$, however, evaporation rates exceed this rate by approximately 60 cm $year^{-1}$ (Simms et al., 2010). The combination of the rate of evaporation when compared to precipitation, and the isolated nature of the bay, result in hypersaline conditions with average salinities ranging from about 40 to 50 (Simms et al., 2010). During approximately seven months of the year strong winds from the southeast continuously blow across Baffin Bay at an average of 15 to 24 km h^{-1} (Simms et al., 2010). As a result, the circulation of water in Baffin Bay is primarily wind driven as it is a microtidal system, and the residence time of the water typically exceeds a year (Smith, 1977).

B. Sampling and field measurements

Surface water samples were collected monthly at nine sampling sites located throughout Baffin Bay from November 2015 to November of 2016. [Table 3]. All samples were collected in 125-mL HDPE bottles that have been rinsed with acid, rinsed with type I water as specified by ASTM

D1193, ISO 3696, and CLSI-CLRW standards (Resistivity of < 18 (MΩ-cm) at 25 °C and Total Organic Carbon (TOC) < 50 (ppb)), and finally triple rinsed in the surface water sample. Samples were placed on ice until filtered through a 0.2 μm GF/F and frozen.

Site Name	Latitude	Longitude
Site 1 (Drum Point-Cayo del Grullo)	27.36793	-97.7024
Site 2 (Site 55- Laguna Salada)	27.26858	-97.7226
Site 3 (Marker 36)	27.27725	-97.6249
Site 4 (Alazan Mouth)	27.27672	-97.5821
Site 5 (Petronila-Alazan)	27.35265	-97.5154
Site 6 (Marker 14)	27.26562	-97.4937
Site 7 (South Marker)	27.26542	-97.4197
Site 8 (Middle Mouth- Marker 2)	27.27767	-97.4129
Site 9 (North Mouth)	27.32025	-97.4099

Table 3. Table of Baffin Bay sites and their geographical coordinates.

C. NO_3^-, NO_2^-, NH_4^+, and TDN concentration analysis.

The Nr concentration analysis was conducted by the TAMU-CC Estuarine and Coastal Ecosystems Dynamics Lab after being filtered through 0.7 μm GF/F. Nitrate (NO_3^-), nitrite (NO_2), and ammonium (NH_4^+) concentrations were analyzed on a Seal QuAAtro Autoanalyzer using Standard Method 4500-NO3 F (for NO_2^- and NO_3^-) and Standard Method 4500-NH3 G (for NH_4^+). TDN concentration was determined using a Shimadzu TOC-V analyzer with nitrogen module according to the American Society for Test Methods D5176. The DON concentrations in Baffin Bay were determined by subtracting the concentration of DIN (i.e. NO_3^-, NH_4^+, and the sum of NO_3^- and NO_2^- (N+N)) from the TDN concentration.

Following the initial concentration analysis conducted by the TAMU-CC Estuarine and Coastal Ecosystems Dynamics Lab, TDN concentrations were measured again after filtering through a 0.2 μm GF/F to filter out remaining bacteria. Persulfate oxidation and subsequent

cadmium reduction were performed as referenced in Tsunogai et al., 2008.

D. $\delta^{15}N$ of NO_3^- and NO_2^-

The isotopic composition of NO_3^- and NO_2^- was determined as $\delta^{15}N\text{-}N_2O$ using the denitrifier method in combination with a continuous flow isotope ratio mass spectrometer (CF-IRMS) (Sigman et al., 2000). Although NO_2^- is present in the concentration of TDN in Baffin Bay, it is an intermediary in nitrification, and consequently is typically present at very low concentrations (92% of samples less than 1 μM), and does not have a large effect on the overall TDN concentration (99% of NO_2^- sample concentration < 2% of TDN sample concentration) (Wetz et al., 2017; Hadas et al., 2009). Similarly, NO_3^- is present at low concentrations (98% of samples less than 2 μM) and does not have a large contribution to the TDN concentration (95% of NO_3^- sample concentrations < 2% of TDN sample concentration).

The NO_3^- and NO_2^- isotopes were only measured if the combined concentration (N+N) was greater than 3 μM due to both analytical capabilities (MDL ≥ 2 μM), and low average concentrations throughout the bay (84% of samples have N+N concentrations that are < 3% of TDN concentration). Additionally, if the concentration of N+N was greater than 3 μM, the $\delta^{18}O$ of these samples were also analyzed using the denitrifier method and CF-IRMS in order to further constrain possible Nr sources by using information derived from the $\delta^{18}O$ values. For NO_3^- analysis, internationally recognized standards (USGS34, and USGS35) were run with samples to provide a known $\delta^{15}N\text{-}NO_3^-$ reference for data corrections. Data corrections for $\delta^{18}O$ values were provided by running standards USGS32 and IAEA-N3 (also known as IAEA-NO-3).

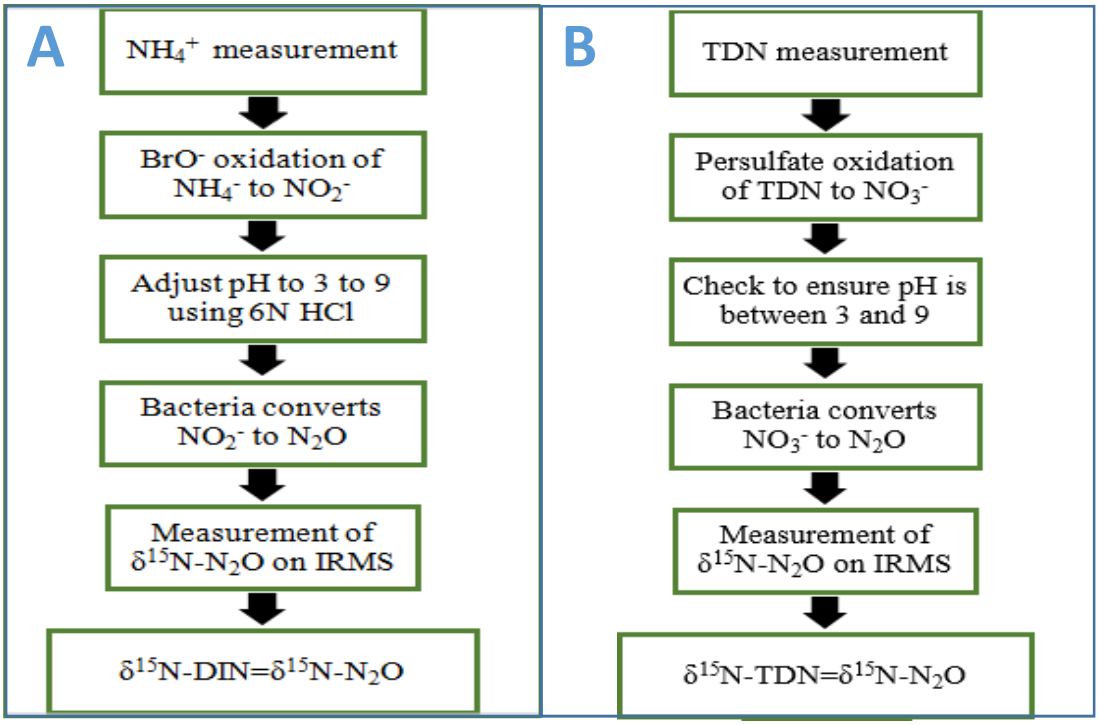

Figure 2. Diagram of methodology used to convert (oxidize) ammonium (Box A) and TDN (Box B) in the Baffin Bay samples to nitrite/nitrate in order to prepare sample for analysis via the bacterial denitrifier method.

E. $\delta^{15}N$-NH_4^+ and Analysis

Because the N+N concentrations are low throughout Baffin Bay, NH_4^+ comprises the majority of the DIN pool (83% of NH_4^+ in samples are >80% of DIN). The NH_4^+ in Baffin Bay samples was oxidized to NO_2^- utilizing the bromate/bromide oxidation method described in Felix et al., 2013 and Zhang et al, 2007 [See Figure 2]. Following oxidation, 12 N hydrochloric acid was added to lower the pH of the oxidized samples to a value between the range of three and nine, as samples with a pH outside of this range would kill the denitrifying bacteria (Felix et al., 2013). Finally, the NO_2^- concentration of the oxidized NH_4^+ in the Baffin Bay samples was measured to determine the efficiency of the conversion of NH_4^+ to NO_2^- (average of 99.5% conversion efficiency). Additionally, USGS isotope standards (USGS 25 ammonium sulfate and USGS 26 ammonium

sulfate) were oxidized along with the samples and included for isotope analysis to provide the isotope laboratory with a reference material with which to correct the resulting isotope data. It should be noted that the results of Zhang et al., 2007 showed that certain forms of DON with differing molecular structures may be oxidized along with NH_4^+ which has the potential to introduce interferences when measuring $\delta^{15}N$. However, supplemental data showed that oxidation yields of twelve relatively low molecular weight representative DON compounds had an average of 8.6% and are not likely to significantly skew the data (Zhang et al., 2007).

F. $\delta^{15}N$ of TDN Analysis

The TDN of the samples was oxidized to NO_3^- using the persulfate method as described in Tsunogai et al., 2008 [See Figure 2]. Each sample was duplicated so that one sample was preserved for isotopic analysis and the other was used to check for the TDN concentration. The duplicate samples were further reduced to NO_2^- via the cadmium reduction method as described in Tsunogai et al., 2008, and the NO_2^- the colorimetric method as described in the Standard Method 4500-NO3 is applied to these samples to determine the TDN conversion efficiency. Representative DON standards (i.e. urea, glycine, EDTA, N-acetyl-D-glucosamine) are oxidized along with the Baffin Bay samples to ensure at least 90% conversion of TDN to NO_3^- from the persulfate oxidation (average oxidation efficiency of 99.8% for all standards) (oxidation efficiency is discussed in more detail in section 2.6).

For this analysis, the persulfate working reagent was mixed using ultrapure High-Performance Liquid Chromatography (HPLC) Grade water. The average blank concentration is 11.4 μM ± 5.8 μM, and since a relatively small amount of persulfate working reagent (0.15 mL) is added to the Baffin Bay samples the overall blank effect is minimal. Additionally, because the average DON

concentrations are high (77 ± 16.5 μM (filtered through 0.7 μm GF/F) and 41.8 ± 13.4 μM (filtered through 0.2 μm GF/F)) the contribution of the blank is only a small fraction in comparison to the total concentration (average blank percentage: 0.3% ± 0.4%), but was not accounted for in calculations due to its negligible influence. After the persulfate oxidation, isotopic analysis was completed as described above.

The δ^{15}N-DON value was isolated from δ^{15}N-DIN by using the isotope mass balance equation: δ^{15}N-TDN= f(δ^{15}N-DIN) + f(δ^{15}N-DON) where f stands for the fraction of the concentration of the respective DIN/DON contributing to the TDN concentration of the sample.

G. NH_4^+ and TDN Oxidation Efficiencies

The concentrations for the Baffin Bay samples were filtered using a 0.7 μm GF/F, at the time of sampling, and then filtered through a 0.2 μm GF/F immediately after being received by the Felix Research Laboratory, and subsequently stored in the freezer prior to oxidation. To ensure that the Nr concentration of the samples were fully oxidized and there was minimal fractionation of the samples, multiple standards were included, and held to an average concentration recovery (post-oxidation/reduction) of 90% or higher. The concentrations of the standards (25 μM, 50 μM, and 75 μM) were chosen in order to bracket the representative concentration range of the Baffin Bay samples observed during the study period. The standards chosen for the TDN persulfate oxidation method included urea (99.6% recovery average), glycine (99.2% recovery average), EDTA (105.5% recovery average), and N-acetyl-D-glucosamine (94.9% recovery average). Urea was chosen as a standard because is it a form of DON that is common component used in fertilizers and has been shown to contribute approximately 50% of the Nr utilized in many coastal regions (Bronk et al., 2002). Glycine was chosen as a standard to represent the dissolved free amino acid

(DFAA) portion of the DON pool, which has been found to comprise approximately 1.2 to 12.5% of the total DON pool (Bronk et al., 2002). The N-acetyl-D-glucosamine was chosen as a standard because studies have shown that this biopolymer is representative of the N-acetyl amino polysaccharides (N-AAPs) and degrades more rapidly in comparison to the more refractory pool of DON, and are important contributors to the semi-labile pool of DON (N-AAPs can comprise ~40 to 50% of surface ocean high molecular weight dissolved organic matter (HMWDOM) (Aluwihare et al., 2005)). The standard concentrations chosen for NH_4^+ (2.5 μM (100.6% recovery average), 5 μM (100.1% recovery average), and 10 μM (97.9% recovery average) were of a representative range of concentrations of ammonium in Baffin Bay. Additionally, two USGS isotope standards (USGS 25 ammonium sulfate (98.4 % recovery average) and USGS 26 ammonium sulfate (98.2% recovery average) were oxidized along with the standards and samples are included for isotope analysis to provide the isotope laboratory with a reference material with which to correct the resulting isotope data.

H. Photo-ammonification Methodology

A surface water sample was collected from Baffin Bay using a 1-liter amber glass bottle in both June 2017 and May 2017. Samples were filtered through a 0.2 μm GF/F and frozen. A control sample was created by pipetting 50 mL of the sample into a 50-mL quartz flask and covering the flask entirely in tin foil. This covered flask was then placed in a solar simulator with UVA340 bulb (Q-panel) as a control sample to ensure that resulting reactions occur due to light rather than temperature. The environment within the solar simulator emits a spectral output similar to that of natural sunlight (295nm to 365nm) and the control sample remains in the solar simulator for 24 hours. Samples were then put in the solar simulator and taken out at various time points and

measured for NH_4^+ concentrations. The first sample was placed into a 50-mL plastic vial and frozen to preserve a sample that was not altered by the solar simulator (0-hour sample) For the remaining samples 50 mL of sample was placed in individual quartz flasks and placed in the solar simulator for 1 hour, 2 hours, 3 hours, 4 hours, 5 hours, 6 hours, 12 hours, and 24 hours. The NH_4^+ concentrations of the various data points were then measured using the ammonium concentration analyses as described in Holmes et al., 1999.

I. Nitrogen Source Dataset

The Nr source samples collected included rainwater, wastewater treatment facility effluent, porewater, cow manure, and synthetic fertilizer. All water samples were prepared for isotopic analysis via the bromate/bromide oxidation method and persulfate oxidation (Tsunogai et al., 2008, Felix et al., 2013, Zhang et al, 2007). The rainwater was collected with an N-Con ADS/NTN wet deposition collector (Model 00-120-2), 0.2 μm filtered immediately at the culmination of each deposition event and then refrigerated until analysis. The Oso Wastewater Treatment Plant sample was collected using an acid-washed 150-mL HDPE bottle, and triple rinsed with sample water before being filtered through a through a 0.2 μm GF/F and frozen until analysis. The cow manure was collected from a grazing pasture located in Long Mott, Texas, and oven dried before being homogenized using a mortar and pestle and subsequently analyzed via Elemental Analyzer (Costech Elemental Combustion System), which is connected to a Thermo Fischer Conflow IV and Delta V Plus IRMS. The synthetic fertilizer (Bumpericrop; total nitrogen content 13%; urea and ammonium sulfate) was homogenized using a mortar and pestle before analysis on the EA-IRMS. Baffin Bay POM $\delta^{15}N$ data was provided by Emily Cira and Dr. Michael Wetz (Cira, unpublished data). Baffin Bay porewater samples were collected using a piezometer, frozen upon

collection, and then filtered through a 0.2 μm GF/F before oxidation and subsequent isotope analysis.

Solid Source $\delta^{15}N$ Values	$\delta^{15}N$ Values	Source
Particulate Organic Matter	4.93 ± 1.05‰	Cira, unpublished data
Synthetic Fertilizer	-0.60 ± 0.26 ‰	TAMU-CC Isotope Core Laboratory
Manure	3.90 ± 0.18 ‰	TAMU-CC Isotope Core Laboratory

Table 4. Table of $\delta^{15}N$ values for representative sources of Nr around the Baffin Bay region.

J. Statistics

A correlation plot was created in order to determine significant relationships between both the explanatory and dependent variables (Appendix H). Additionally, to determine the variables in Baffin Bay that had the greatest effect on $\delta^{15}N$-TDN values, a linear model was generated for all the months combined with $\delta^{15}N$-Nr values as the dependent variable and various monthly environmental variables as the independent variables (Appendix J).

Linear Model	Adjusted R-Squared	F-statistic	p-value
39.69 -(0.31*Chlorophyll a) + (0.02*DOC μM) – (0.44*NH4+ μM) - (5.51*Orthophosphate) – (1.02*Precipitation) – (1.44*Salinity) + (0.52*temperature) – (0.33*δ15N-DON)	0.5476	8.868	3.925e-07
50.81 - (0.44*Chlorophyll a) + (0.01*DOC μM) – (0.52*NH4+ μM) - (6.25*Orthophosphate) – (0.98*Precipitation) + (0.04*Silicate) – (1.76*Salinity) + (0.56*temperature) – (0.34*δ15N-DON)	0.5615	8.40	4.271e-07

Table 5. Table displaying formula for the top two linear models of the most significant explanatory variables for the dependent variable δ^{15}N-DIN including Adjusted R-squared, F-statistic, and p-value.

Linear Model	Adjusted R-Squared	F-statistic	p-value
6.93- (0.13*DON μM) + (0.27*NH_4^+ μM) - (0.20*δ^{15}N-DIN) + (1.08* δ^{15}N-TDN)	0.5179	15.5	2.599e-08
6.54 - (0.13*DON μM) + (0.26*NH_4^+ μM) - (0.20*δ^{15}N-DIN) + (1.06* δ^{15}N-TDN) + (0.78*Orthophosphate)	0.523	12.84	5.405e-08
1.74 + (0.01*DOC) - (0.14*DON μM) + (0.34*NH_4^+ μM) - (0.16*δ^{15}N-DIN) + (0.94* δ^{15}N-TDN) - (2.32*NO_2^- μM) +(0.41* NO_3^- μM)	0.5492	10.4	8.393e-08

Table 6. Table displaying formula for the top three linear models of the most significant explanatory variables for the dependent variable δ^{15}N-DON including Adjusted R-squared, F-statistic, and p-value.

These environmental variables include ammonium concentrations, DON concentrations, nitrate concentrations, nitrite concentrations, chlorophyll a, silicate, dissolved organic carbon (DOC), orthophosphate, temperature, salinity, and precipitation. The models were dredged and, in order to evaluate the model that best fits the data, their Akaike Information Criterion (AICc) values were compared. Each linear model then was assessed by the adjusted R-squared values, the p-value of both the model and the variables included within the model, and the plot of the residuals. Additionally, a principle component analysis using was performed on all environmental variables, excluding DOC and silicate because these variables masked the results of the other variables (Appendix K).

CHAPTER III- RESULTS AND DISCUSSION

A. DIN concentration and isotopic composition

1. DIN seasonal variations

The samples that have combined NO_2^- and NO_3^- (N+N) concentrations above 3 μM were analyzed for their isotopic composition (n = 10) [Table 7]**.** Additionally, the isotopic composition of the $\delta^{18}O$ of the elevated N+N samples was measured. Dual isotope measurements of $\delta^{15}N$ and $\delta^{18}O$ have been used in previous studies to constrain and differentiate between multiple sources with similar $\delta^{15}N$ values as well as evaluate possible processing effects (Burns et al., 2009, Wankel et al., 2009, Wankel et al., 2006, Lehmann et al., 2004). For example, during denitrification, a process where NO_3^- is being converted to N_2, the $\delta^{15}N$ and $\delta^{18}O$ are both affected by the fractionation effect associated with denitrification which typically results in a 1:2 change in O^{18}-NO_3^-:$\delta^{15}N$-NO_3^- of the residual NO_3^- pool (Burns et al., 2009, Kendall et al., 2007). Using this dual isotope approach aids in determining where this elevated N+N originated and how it is being processed.

Sample Date	Sample Site	NO_2^- (μM)	NO_3^- (μM)	(N+N) (μM)	$\delta^{15}N$-N+N Values (‰)	$\delta^{15}N$-NH_4^+ Values (‰)	$\delta^{18}O$ values (‰)
Jan-16	Site 5	0.37	4.20	4.57	16.44	-19.71	23.56
Mar-16	Site 1	5.75	8.04	13.78	6.58	2.92	9.15
Mar-16	Site 2	3.10	2.03	5.13	2.40	5.71	8.34
Mar-16	Site 5	8.16	40.32	48.48	3.67	-6.01	10.64
May-16	Site 5	1.51	22.85	24.36	9.97	-20.72	13.01

July-16	Site 5	3.68	0	3.68	5.29	-10.07	12.76

Table 7. Table of date, location, and isotope values for Baffin Bay samples with N+N concentrations exceeding 3μM.

Most samples with elevated N+N occurred in spring months, which is consistent with forms of DIN being loaded into Baffin Bay during rain events. Since atmospherically derived nitrate typically has a high $\delta^{18}O$ signature (+65 to +95‰) the N+N samples in Baffin Bay are showing influences from sources other than atmospheric deposition, as the $\delta^{18}O$ values of the N+N samples (8.3‰ to 23.6‰) do not fall within these ranges (Hastings et. al, 2004; Kendall, 1998). It is possible N+N derived from atmospheric deposition and an alternative source of N+N with lower $\delta^{15}N$ and $\delta^{18}O$ values are mixing. This is supported by the typical isotope signature of synthetic fertilizers (fertilizer $\delta^{15}N\text{-}NO_3^-$: −5 to +8‰ and $\delta^{18}O$: +15 to +25‰) which could have been loaded into Baffin Bay via runoff during the spring months (Singleton et al., 2007, Kendall, 1998). Additionally, in January the $\delta^{15}N$-N+N and $\delta^{18}O$ values are relatively elevated when compared to the average $\delta^{15}N$ (5.6‰ ± 3‰) and $\delta^{18}O$ (10.8‰ ± 2.1‰) of the sites (increase of ~9.1‰ ($\delta^{15}N$-N+N) and ~10.7‰ ($\delta^{18}O$)). These ranges of $\delta^{15}N$ and $\delta^{18}O$ and fall close to the isotopic range of manure and sewage-derived NO_3^- ($\delta^{15}N\text{-}NO_3^-$: +10 to +25‰ and $\delta^{18}O$: -5 to +15‰). This is a reasonable explanation as in January 2016, there was relatively low rainfall (2.20 inches) [See Figure 3]. The higher $\delta^{18}O$ value of ~25‰ per mil in January exhibits the influence of either the contribution of a source of nitrogen with a relatively high $\delta^{18}O$ such as synthetic fertilizers (+17 to +25‰) or atmospheric deposition (+65 to +95‰). Alternatively, the higher $\delta^{18}O$ value observed in January could also be due to a fractionating process such as denitrification, nitrification, or phytoplankton assimilation. Due to the limited rainfall in January and lack of nutrient input due to runoff, the elevated $\delta^{18}O$ value during this month is likely due to a fractionating process.

Denitrification is likely the culprit, as the $\delta^{15}N$ and $\delta^{18}O$ values in January appear to be coupled as the values in January are approximately double the average of the remainder of the $\delta^{15}N$ and $\delta^{18}O$ values observed. Though denitrification produces a $^{15}\varepsilon:^{18}\varepsilon$ of 2:1, it has been shown that denitrification can also result in a $^{15}\varepsilon:^{18}\varepsilon$ of 1:1 (Wankel; et al., 2009, Kendall et al., 2007, Granger et al., 2004).

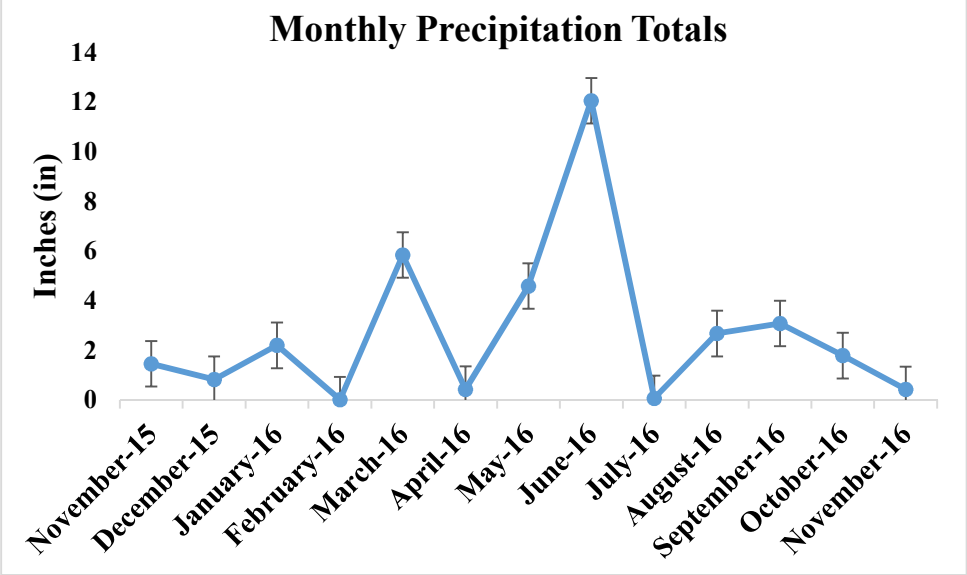

Figure 3. Line graph showing monthly precipitation totals for Baffin Bay throughout the study period.

The contribution of sewage-derived N+N is reasonable because Baffin Bay receives little riverine input throughout the year due to dry conditions. The contribution of sources of Nr to Baffin Bay is dependent on hydrological conditions, and it has been observed that the riverine tributaries that feed into the branches of Baffin Bay can become stagnant during dry conditions or droughts (Wetz et al., 2017). It is during these dry months that more consistent flows such as wastewater effluent or septic systems may have a greater contribution on Nr inputs and $\delta^{15}N$ values than other external inputs of Nr such as runoff, atmospheric deposition, and riverine inputs (Wetz et al., 2017).

The highest concentrations of NH_4^+ occur in the months November 2015 (9.5 ± 10.4 μM), March (10.4 μM ± 11.3 μM), May (10.7 μM ± 7.5 μM), July (8.4 μM ± 5.9 μM), and August (9.0 μM ± 7.0 μM) (See Figure 4). The widest range of concentrations across sites occurred in March (2.2 μM to 32.5 μM) and November 2015 (1.2 μM to 27.3 μM). When separated for analysis by season (winter (December, January, February), spring (March, April, May), summer (June, July, August), and fall (September, October, November)) average NH_4^+ concentrations were highest in the spring (8.5 μM ± 1.6 μM) followed by the summer (7.3 μM ± 1.2 μM), fall (3.6 μM ± 0.5 μM), and winter (3.6 μM ± 0.3 μM).

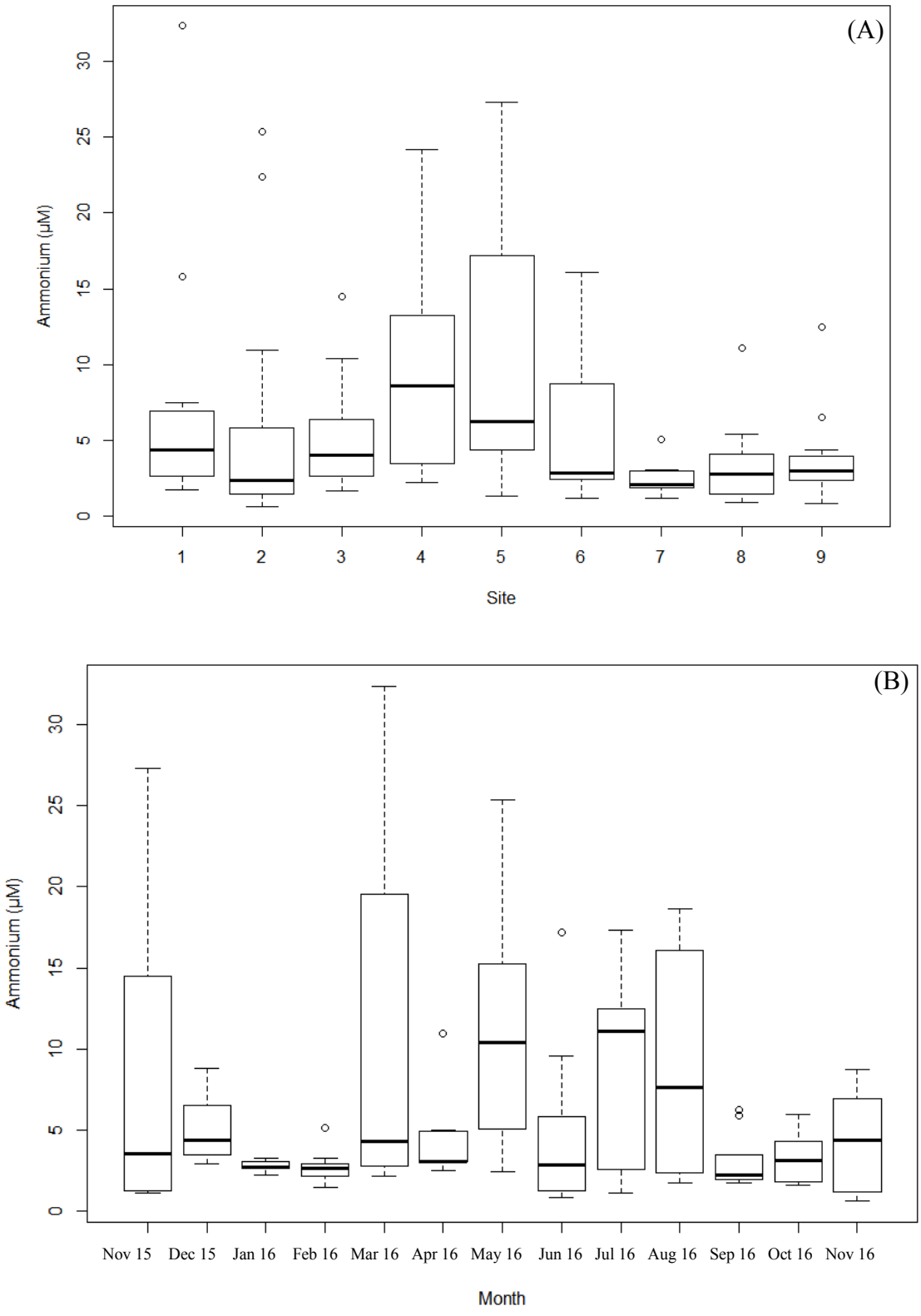

Figure 4. Panel A shows box plot of NH_4^+ concentrations by site and Panel B shows box plots of NH_4^+ concentrations by month.

These trends are supported by the loading of inorganic nutrients into Baffin Bay during the months with the greatest amounts of precipitation (Wetz et al., 2017; Ockerman and Petri, 2011; Gardner et al., 2006; Seitzinger at al., 2002). Rainfall data obtained from a weather station in Kingsville, Texas (Station ID: USW00012928) located approximately 3.5 miles northeast of the mouth of Cayo de Grullo recorded 12.6 inches of rainfall during the month of June in 2016. This was the largest rainfall event at Baffin Bay during the study period [See Figure 3]. When separated into seasons, the winter and fall months had the smallest rainfall totals (DJF: 3.0 in ± 1.1 in, SON 5.3 in ± 1.3 in) while the spring and summer months had the largest rainfall events (MAM: 10.9 in ± 2.8 in, JJA: 14.8 in ± 6.3 (in)). Given that Baffin Bay does not receive large continuous amounts of freshwater inflow throughout the year, the run-off from rain episodes contributes greatly to the nutrient inputs to Baffin Bay (Ockerman and Petri, 2011; Wetz et al., 2017). The lowest concentrations of NH_4^+ occurred in September (3.2 μM ± 2.0 μM) and in January (2.8 μM ± 1.1μM) and February 2016 (2.7 μM ± 0.3 μM), all of which had little reported rainfall.

The seasonal variations in δ^{15}N-DIN (which is predominately representative of δ^{15}-NH_4^+ due to low ambient N+N concentrations throughout much of the study period) values throughout the year show relatively steady isotope value averages in both the winter (δ^{15}N-DIN 5 ± 5‰) and spring (3.7 ± 6‰) [See Figure 5][See Figure 6]. A possible explanation for the lowering of the average δ^{15}N values from the winter to the spring could be due to the mixing of a source of DIN with a lower δ^{15}N signature being introduced by the rainfall events in the spring such as atmospheric deposition (-15‰ to +15 ‰) or synthetic fertilizers (-2‰ to +2‰) (Kendall et al., 2007; Choi et al., 2017) [See Figure 3]. The influence of a source such as synthetic fertilizers is reasonable as the primary land use of the Baffin Bay watershed is agricultural land (~33% cropland and 64% rangeland) (Ockerman and Petri, 2011).

During the late summer isotopic values decreased (summer average value of δ^{15}N-DIN: -1.6 ± 4 ‰ or a decrease of ~6 ‰) while the NH_4^+ concentrations decreased only slightly (summer NH_4^+ concentration: 7.5µM ± 2µM) [See Figure 5]. The pattern of isotopically low δ^{15}N-DIN in the summer likely indicates the production of isotopically light NH_4^+ via photo-ammonification. This idea is supported by the depletion of DON concentrations as well as a relatively high isotope values (average δ^{15}N-DON: 12.5 ± 6‰) for the summer months [See Figure 10].

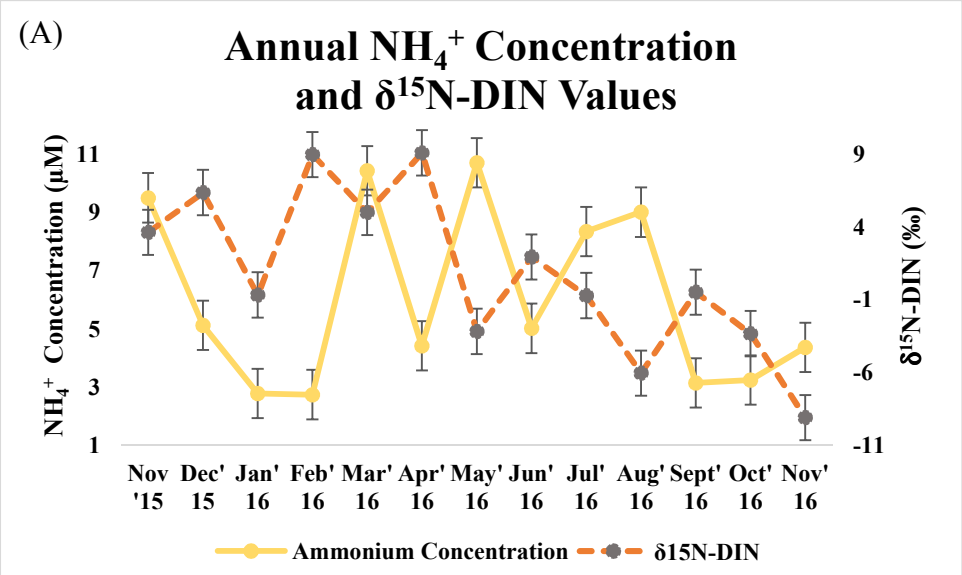

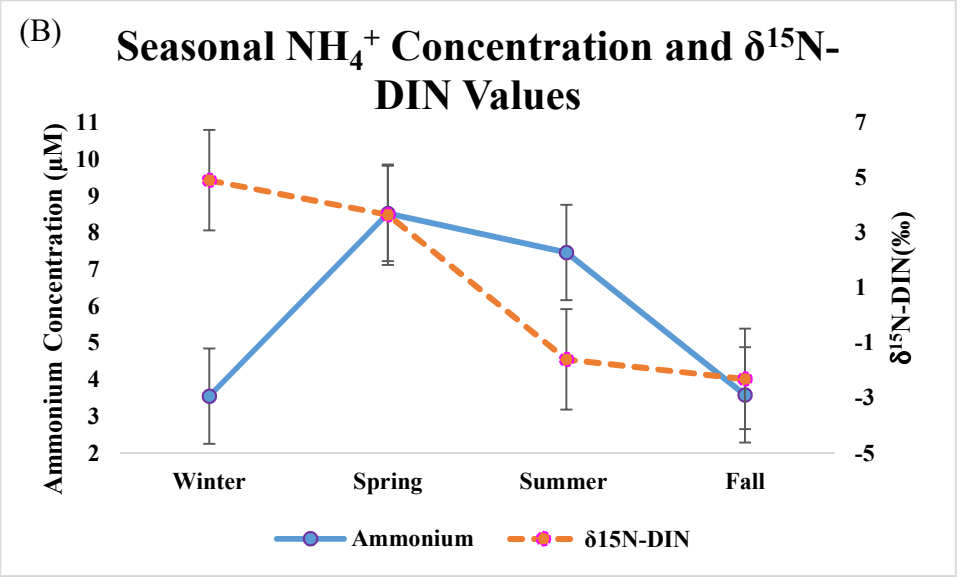

Figure 5. Panel A: View of annual NH_4^+ concentrations and $\delta^{15}N$-DIN values. Panel B: View of seasonal NH_4^+ concentrations and $\delta^{15}N$-DIN values.

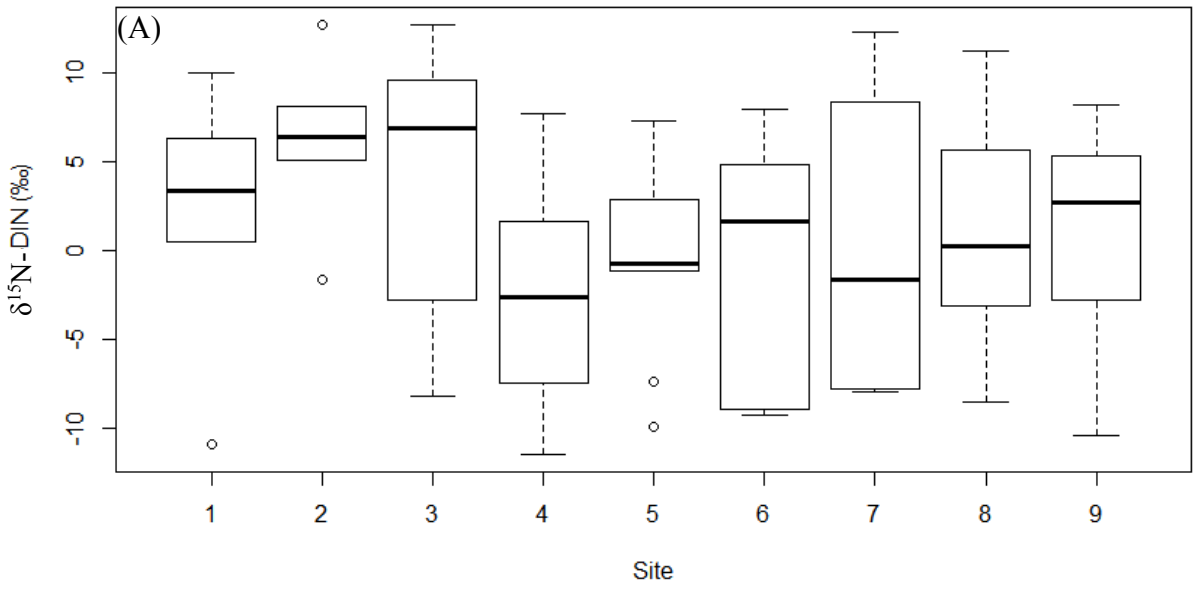

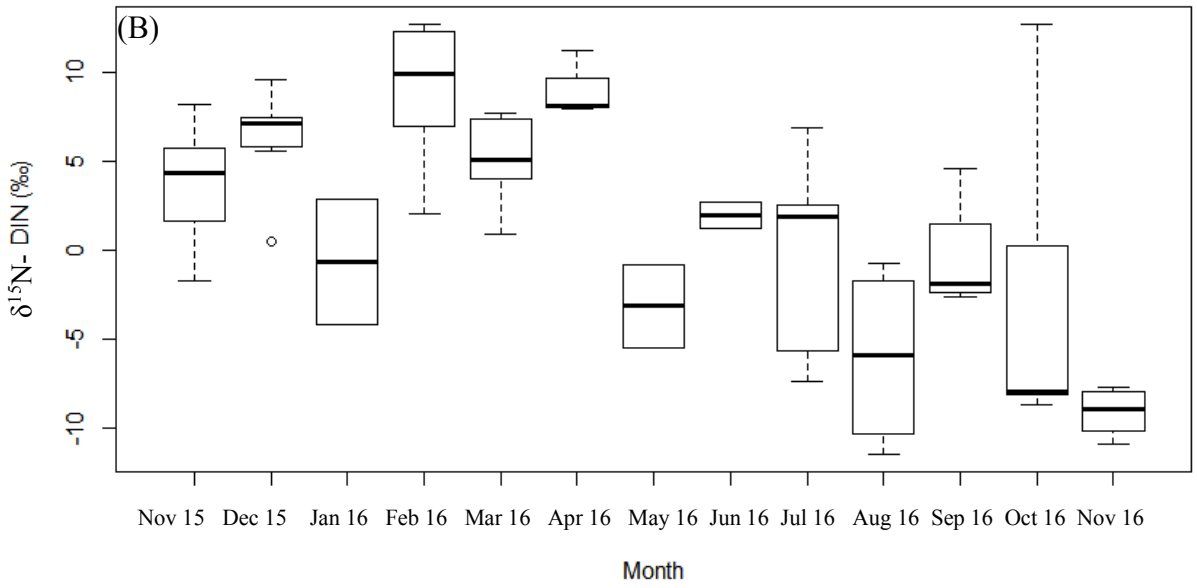

Figure 6. Panel A shows box plot of δ^{15}N-DIN values by site and Panel B shows box plots of δ^{15}N-DIN values by month.

2. DIN spatial variations

The range of NH_4^+ concentrations from November 2015 through November 2016 was from 0.6 µM to 32.4 µM for NH_4^+ and the average concentration was 5.9 ± 6.2 µM (NH_4^+). The highest average concentrations and ranges of NH_4^+ occur in Sites 4 (Alazan Mouth) (9.3 µM ± 6.8 µM) and 5 (Petronila (Alazan) (10.0 µM ± 8.1 µM). The sites with the most extreme outliers of NH_4^+ concentrations were Site 1 (Drum Point-Cayo del Grullo) and Site 2 (Site 55- Laguna Salada) in March and May 2016 [See Figure 4]. A possible explanation for the high average NH_4^+ concentrations in Site 4 is its location in proximity to the freshwater riverine inputs from Los Olmos Creek and San Fernando Creek in the western portion of Baffin Bay. Similarly, the reason for the elevated concentrations of NH_4^+ in Site 5 is likely due to its proximity to the primarily agricultural inputs by Petronila Creek into Alazan Bay (Wetz, 2017; Ockerman and Petri, 2001) [See Figure 7]. This idea is supported by the comparatively low average δ^{15}N-DIN signatures

observed at Sites 4 (mean: -2.3‰,) and 5 (mean: -0.2 ‰,) as isotope signatures associated with agricultural sources such as fertilizer are typically low (-2 to +2 ‰) (Choi et al., 2017) [See Table 1] [See Figure 8].

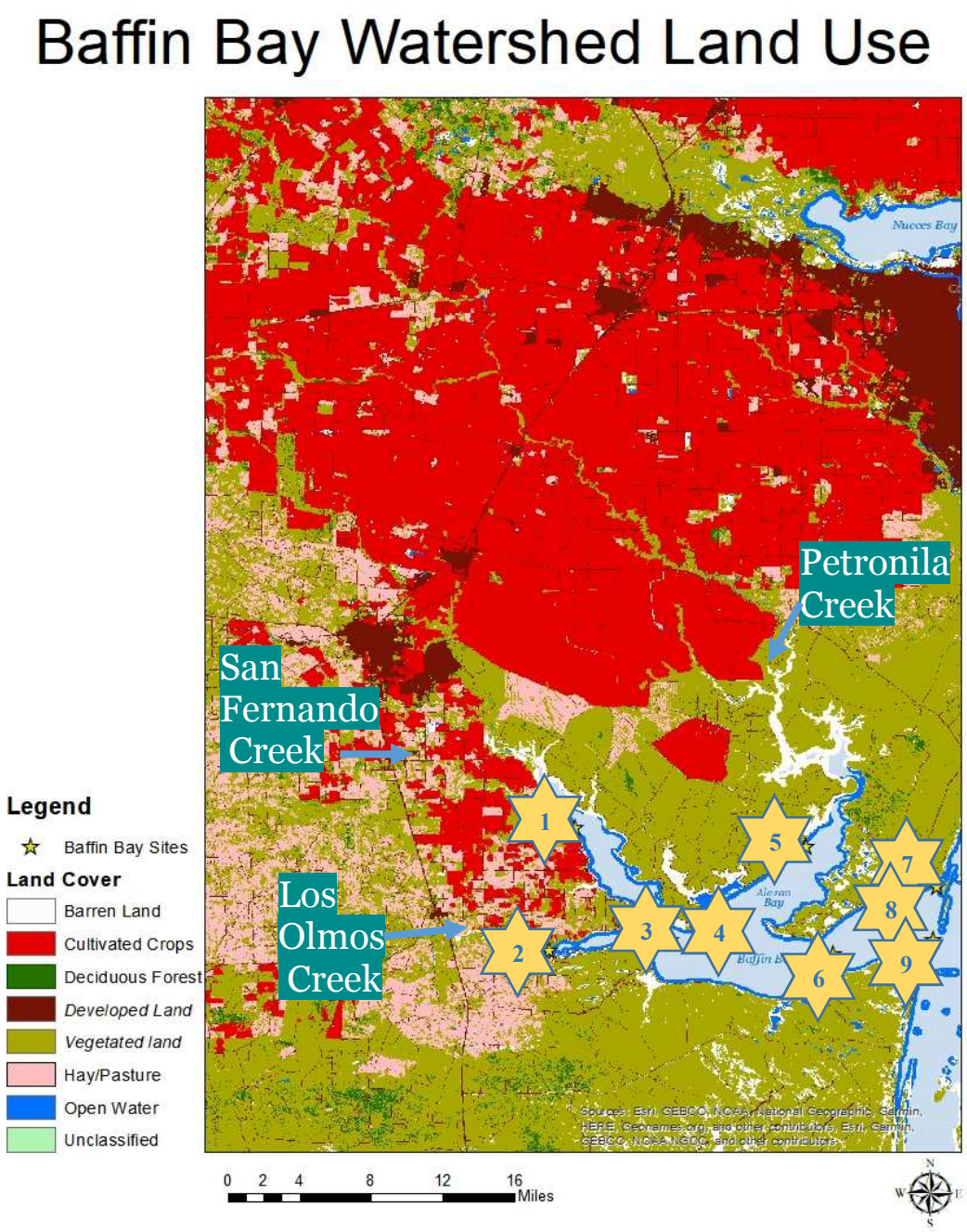

Figure 7. View of land use surrounding Baffin Bay. The stars indicate Baffin Bay Sites and displays the landcovers is primary use as cultivated crops, developed land, and vegetated land.

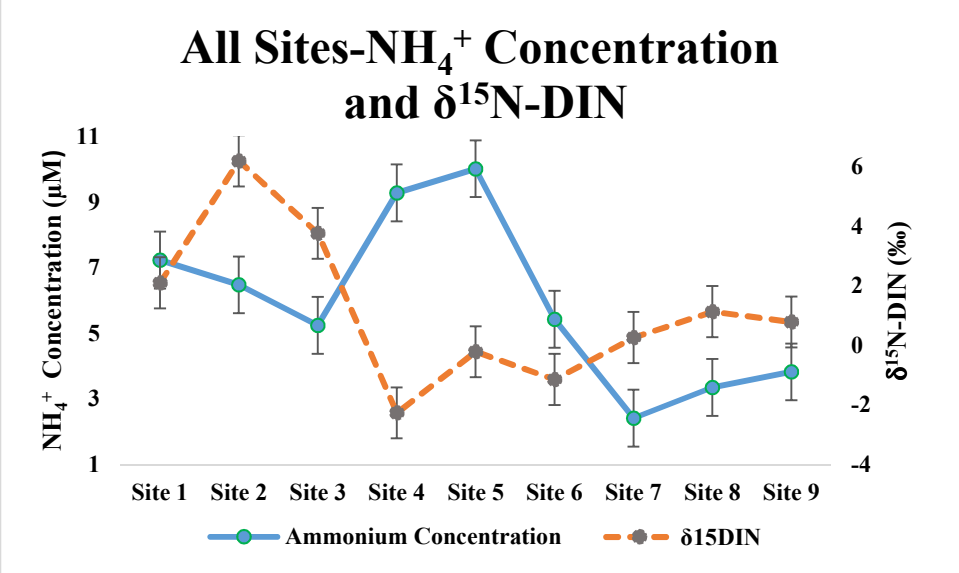

Figure 8. Average annual concentrations of NH_4^+ and average δ^{15}N-DIN values for each Baffin Bay site.

The lowest concentrations of NH_4^+ occur in the sites towards the mouth of the bay; Site 7 (South Mouth) (2.4 µM ± 1.0 µM), Site 8 (Middle Mouth) (3.4 µM ± 2.8 µM), and Site 9 (North Mouth) (3.8 µM ± 3.1 µM) [Figure 4]. This trend is supported by the consumption and assimilation of NH_4^+ concentrations along the salinity gradient as evidenced in previous studies (Avery et al., 2016; Viana and Bode, 2015; Schlarbaum et al., 2010; Glibert et al., 2007; Gardner et al., 2006). This is further supported by the increase of δ^{15}N-DIN from the landward sites (Site 4) to the mouth of the bay (Sites 7- 9). However, Sites 1, 2, and 3 show relatively elevated δ^{15}N-DIN values, possibly indicating the influences of an NH_4^+ source with a high δ^{15}N signature such as wastewater or septic effluent (+5 to + 9‰) (Cole et al., 2006) [See Figure 6]. This could be due to the proximity of Sites 1, 2, and 3 to inputs from San Fernando and Los Olmos Creek [See Figure 7]. Site 1 is downstream of 7 registered wastewater outfall locations, and a wastewater outfall permitted to Kleberg County is located approximately 4.5 miles northwest of Site 3. Additionally, the city of

Riviera (pop. 1,945) has a wastewater outfall registered to the Riviera Water Control & Improvement District located approximately 6.3 miles west/southwest of Site 2 (TCEQ).

B. DON concentrations and isotopic composition

1. DON seasonal variations

The range of DON concentrations after filtration through a 0.7 μm GF/F from November 2015 through November 2016 was from 33.0 μM in May 2016 to 139.7 μM in August 2016 [See Figure 9]**.** The average DON concentration throughout Baffin Bay was 77 ± 16.5 μM. Because phytoplankton and bacteria cell sizes have been recorded down to 0.2 μM and 0.05 μM respectively, it is possible that particulate organic nitrogen was included in the TDN concentration provided by the TAMU-CC Estuarine and Coastal Ecosystems Dynamics Lab because of their ability to pass through the 0.7 μm GF/F filter (Robertson and Button, 1989; Chisholm, 1992; Gasol et al., 1995).

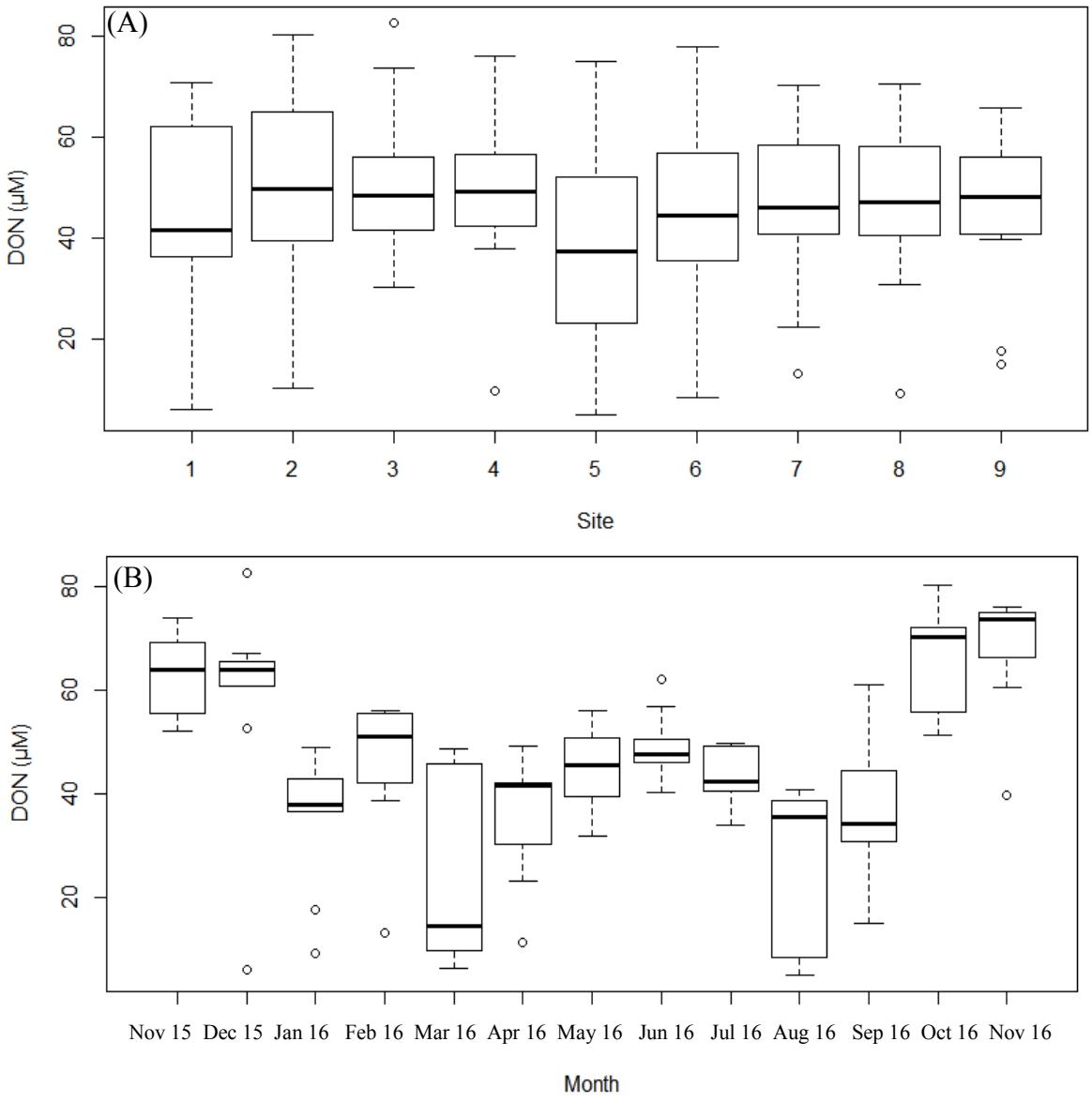

Figure 9. Panel A shows box plot of DON concentrations by site and Panel B shows box plots of DON concentrations by month (filtered by 0.7 µm GF/F).

The DON concentration measured after filtering through a 0.2 µm GF/F and persulfate oxidation for each site had wide ranges, but the median DON concentrations were fairly consistent and had an average concentration of 46.4 µM ± 3.3 µM [See Figure 9]**.** The highest DON concentration throughout the year was observed in December 2015 (82.8 µM) and the highest average concentration was observed in November 2016 (67.8 µM ± 11.7 µM). The widest range

of concentrations were observed in December of 2015 (5.9 μM to 82.8 μM), and the lowest average concentration was observed in March of 2016 (22.9 μM ± 18.9 μM).

Seasonal DON concentrations display a trend of lower average concentrations in the spring and summer (36 ± 13.2 and 40.6 ± 11.7) when compared to the fall and winter (58.3 ± 14.3) [See Figure 10]**.** Seasonal δ^{15}N-DON patterns display a trend of increased values in the spring (average: 12 ± 6‰) and summer (average: 12.5 ± 6‰) when compared to the fall and winter months (10 ± 2.6‰ and 9.5 ± 1.8‰, respectively) [See Figure 10]. δ^{15}N-DON values during these spring months are higher (~2 ‰) compared to the seasonal average. The elevated δ^{15}N-DON observed in the spring is likely due to phytoplankton consumption and assimilation. As phytoplankton will likely preferentially use the lighter isotope of nitrogen (^{14}N) when assimilating nutrients for growth and energy, isotopically enriched DON concentrations would typically remain unless totally consumed. The assimilation of DON by phytoplankton is also supported by a marked decrease in DON concentrations in the spring concurrent with an enrichment in δ^{15}N-DON values. Additionally, the stability of the δ^{15}N-DIN values despite increased concentrations in the spring indicate that organisms at this time are primarily assimilating DON, as assimilation is a highly fractionating process (ε: 9.4‰ ± 6.6‰), which would be reflected in the δ^{15}N-DIN values. This could be due to a lag time between the loading of the typically preferred DIN concentrations during the spring rain events and phytoplankton uptake. An additional factor possibly contributing to the trend of decreasing DON concentrations and the relatively stable δ^{15}N-DIN vales in the spring is the rapid remineralization of DON by bacteria. The warming temperatures may stimulate bacterial degradation of DON, which would contribute to the NH_4^+ concentrations in the spring (Santos et al, 2009). This is supported by the decrease of DON concentrations during the summer.

Additionally, since the remineralization process has a relatively small fractionation effect (± 1‰) the δ^{15}N-DIN values would remain fairly stable.

In the summer, a decrease in DON concentration is observed with a concurrent increase in δ^{15}N-DON, likely attributed to photo-ammonification from the increased exposure of DON to UV radiation, causing degradation (Bushaw et al., 1996 Shiller et al., 2006; Tarr et al., 2001). This processing mechanism is supported by an increase in isotopically light (δ^{15}N-DIN: -1.5 ± 4‰) NH_4^+ concentrations. Additionally, the concentration of chlorophyll a began to decrease from its peak concentration in June (17.8 µg/L) to 10.1 µg/l in August, indicating that this decrease in DON concentrations is not likely due to phytoplankton consumption [See Figure 11]. Finally, the accumulation of DON concentrations observed in the fall is consistent with cell death and phytoplankton exudation of DON towards the end of their growth cycle (Biddanda and Benner, 1997). Evidence for phytoplankton die off is supported by the decrease in average chlorophyll a levels observed in the fall and winter [See Figure 11]**.** Additional support for this trend is the observed decrease of the δ^{15}N-DON values from summer to the fall and winter. The exudation of extracellular products in the form of DON after cell death would be depleted in ^{15}N relative to the δ^{15}N of the phytoplankton (Checkley Jr and Miller, 1989). Additionally, bacterial degradation of the available DON after the phytoplankton biomass die off would contribute to the lower δ^{15}N-DIN values observed in the fall.

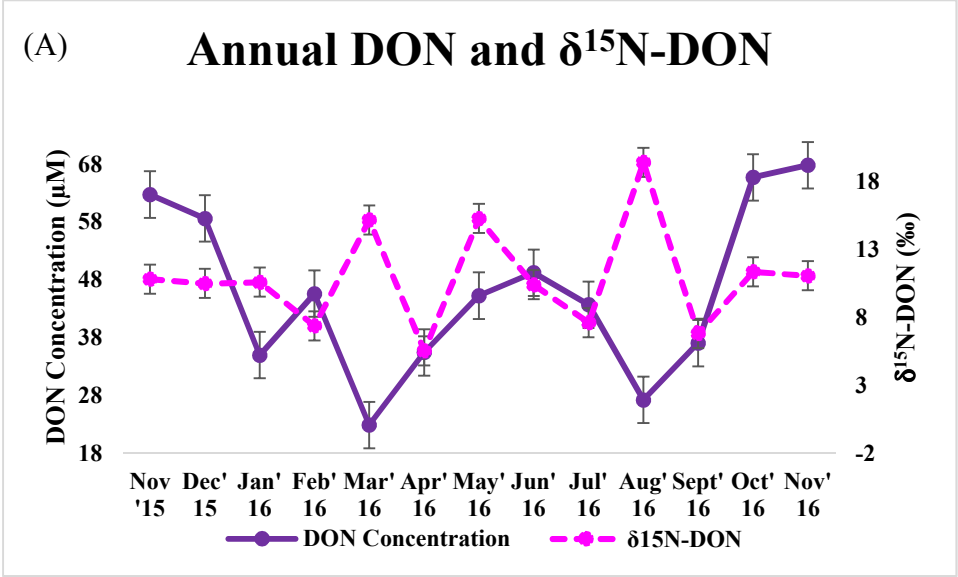

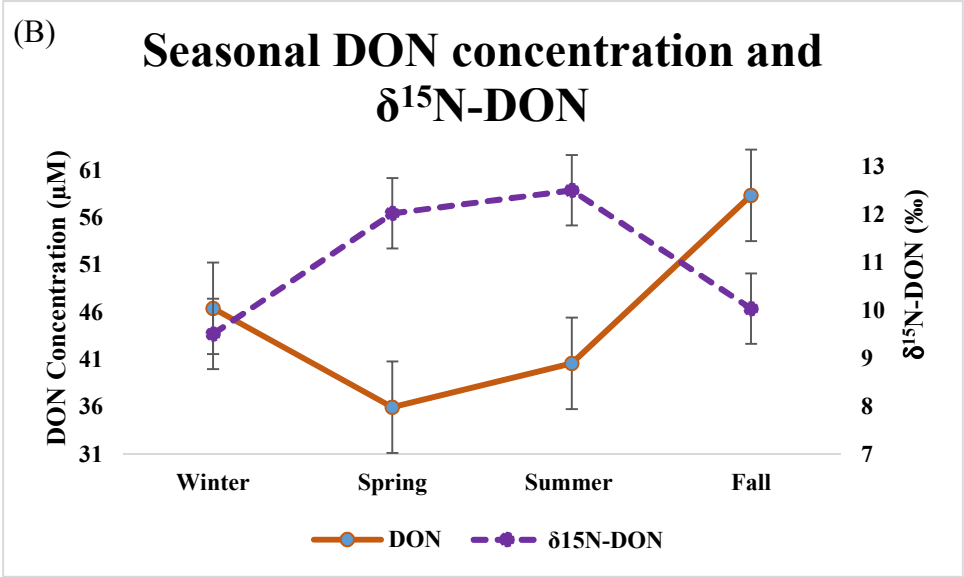

Figure 10. Panel A: View of annual average DON concentrations plotted with annual average δ^{15}N-DON values. Panel B: View of seasonal average DON concentrations plotted with seasonal average δ^{15}N-DON values.

It appears that though DON may be used preferentially in the spring time by phytoplankton, throughout the remainder of seasons DON does not appear to be utilized heavily by phytoplankton communities. This is evidenced by the stability of the concentrations when plotted against seasonal

chlorophyll a levels [See Figure 11]**.** This scenario is additionally supported by lack of a significant correlation between overall chlorophyll a and DON concentrations (Appendix H). This coincides with the fact that the only brown tide blooms that were reported during this study were isolated to Site 2 (Laguna Salada) in November 2015 and early in 2016 (Wetz, personal communication). It is possible that due to environmental factors such as amount of rainfall and salinity levels, that this organism was not present during the majority of the study period.

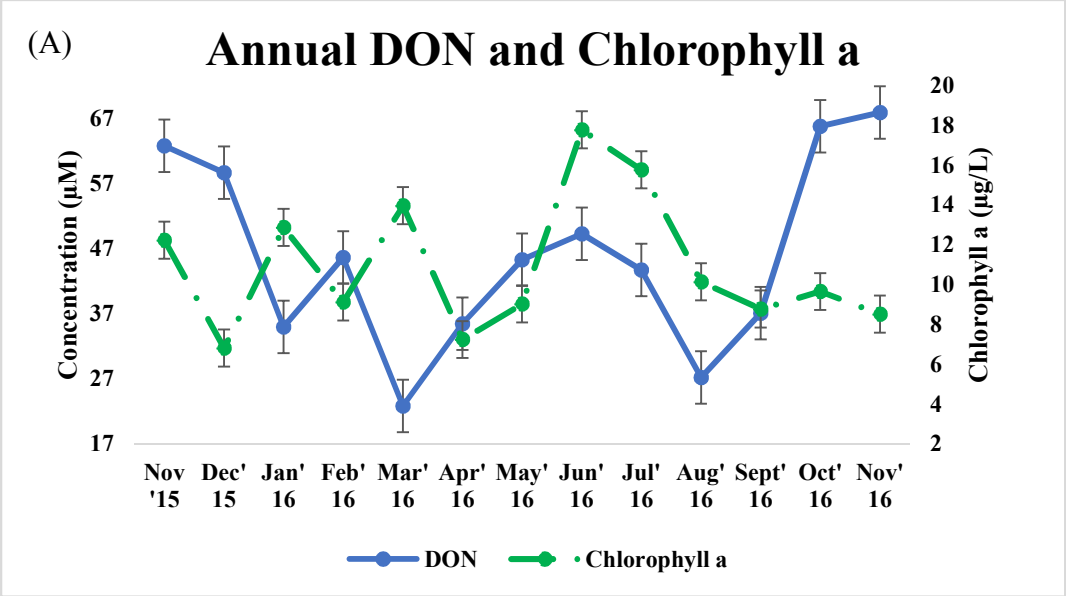

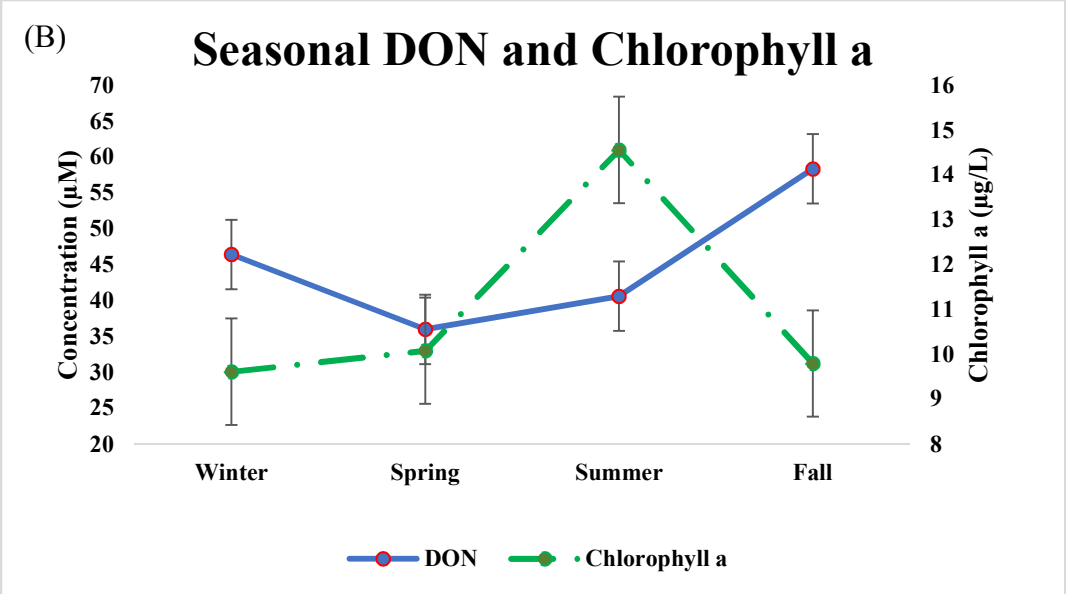

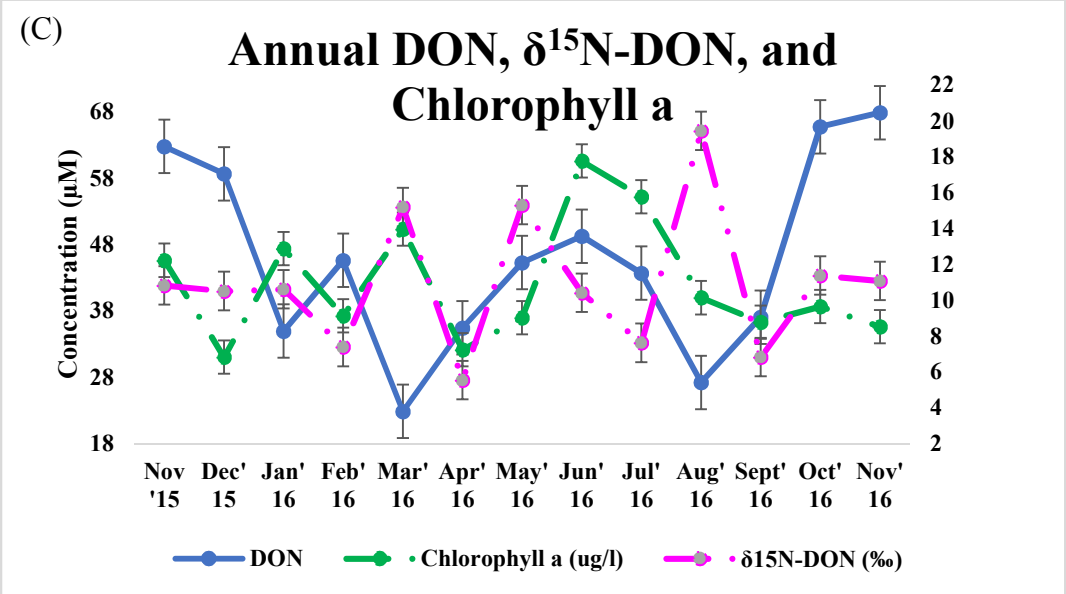

Figure 11. Panel A: View of annual DON concentrations and chlorophyll a levels. Panel B: View of seasonal annual DON concentrations and chlorophyll a levels.

2. DON spatial variations

The concentrations throughout the sites ranged from 4.9 µM in August of 2016 to 82.8 µM in December 2015. Site 3 (Marker 36) had highest average DON concentration (51 µM ± 14.7 µM), and the lowest average concentration was observed at Site 5 (39.2 µM ± 23.3 µM) [See Figure 9].

As mentioned previously, wastewater effluent inputs from Los Olmos Creek, San Fernando Creek, and wastewater outfall located on the southeastern edge of the Cayo del Grullo, may all be contributing to the high DON concentrations observed down the salinity gradient in Site 3, due to the relatively steady contribution to the nutrient inputs during the dry months (Wetz, 2015, Wetz, 2017; Ockerman and Petri, 2001). A review conducted by Pehlivanoglu-Mantas and Sedlak stated that the removal of organic nitrogen from these wastewater treatment plants is often inefficient, and DON can comprise up to 65% of the dissolved nitrogen in these effluents (Pehlivanoglu-Mantas and Sedlak, 2006). The elevated DON concentrations observed in Site 3 throughout the year may be due to its proximity to the Riviera WCID wastewater outfall. This idea is supported by δ^{15}N-DON values at this site (δ^{15}N-DON: 9.7 ± 2.1‰), which would support the idea of an allochthonous source such as wastewater/septic effluent (+10 to +25 ‰) contributing to the elevated DON concentrations as well as the range of isotopic δ^{15}N-DON values observed at this site throughout the study period [See Figure 12] (Silva et al., 2002; Kendall et al., 2007, Nestler et al., 2011). Similarly, Sites 2 and 4, both of which have elevated average DON concentrations compared to sites further down the salinity gradient (Site 2: 50.2 µM ± 20 µM and Site 4: 51 µM ± 15 µM) may be affected by wastewater effluents located upstream. The annual averages of the δ^{15}N-DON values at these sites also support the influence of wastewater and septic effluent (Site 2: 9.7‰ ± 5‰ and Site 4: 11.7‰ ± 3‰).

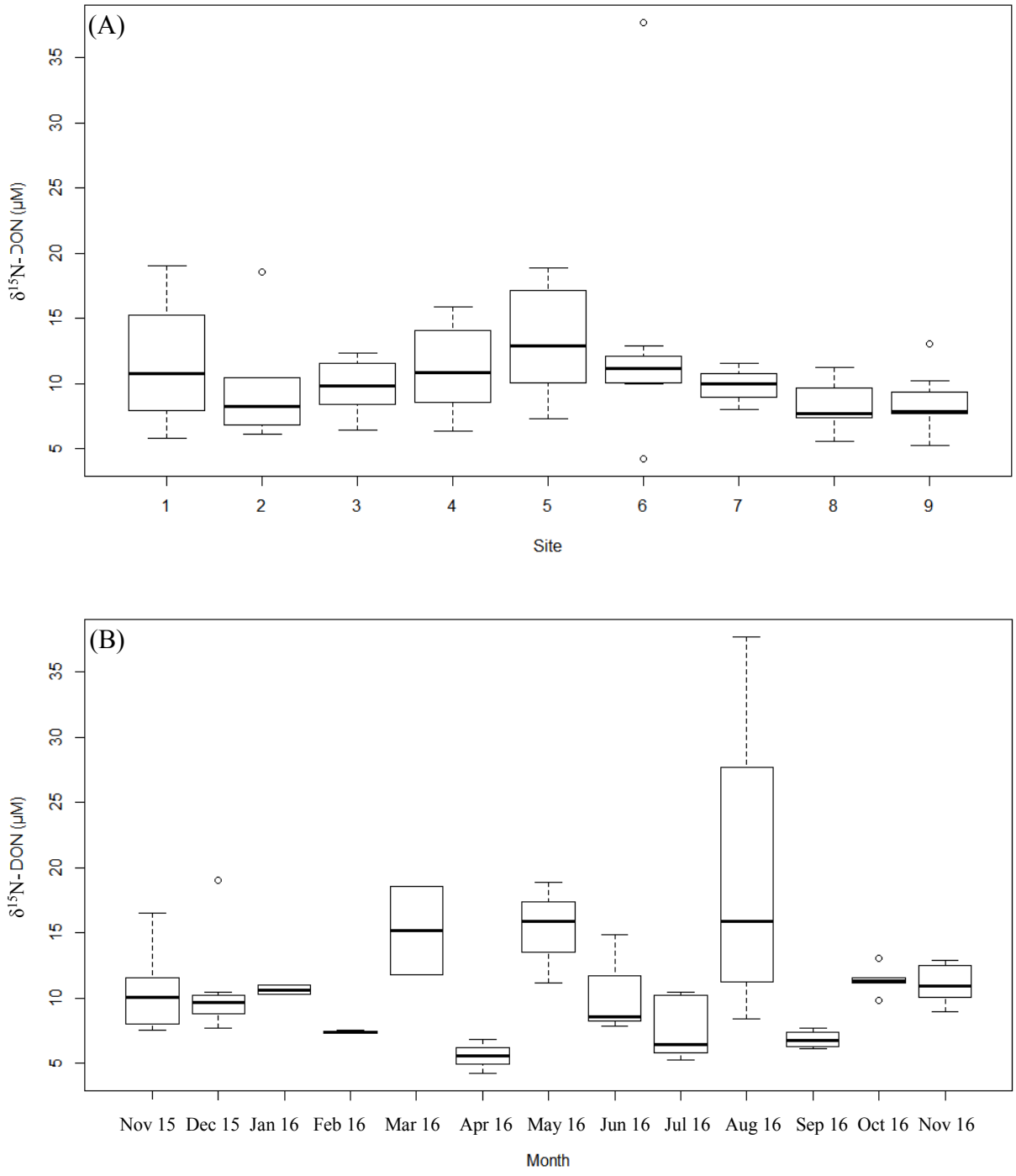

Figure 12. Panel A shows box plot of δ^{15}N-DON values by site and Panel B shows box plots of δ^{15}N-DON values concentrations by month (filtered by 0.2 μm GF/F).

C. Salinity Gradients and Nr Concentration/Isotopic Composition

DON and DIN concentrations were plotted as a function of salinity each month (Appendix C). Since DIN and DON are often introduced via freshwater inputs such as runoff and tributaries, concentrations of DIN and DON are generally greater at the lower end of the salinity gradient, where freshwater is being introduced, and diminishes seawards, as the DIN or DON is either being processed or diluted as the water moves out towards the more saline seawater (Avery et al., 2016; Viana and Bode, 2015; Schlarbaum et al., 2010; Glibert et al., 2007; Gardner et al., 2006). By plotting the DIN/DON concentrations or isotopic compositions as a function of salinity, mixing or production patterns can be observed if the relationship to salinity is either conservative (linear) or non-conservative (non-linear) (Avery et al., 2016, Schlarbaum et al., 2010, Gardner et al., 2006).

For NO_2^- and NO_3^- the statistically significant mixing gradients were observed in March (NO_3^- ; α: 1.09e-05, NO_2^- ; α: 0.001) and May 2016 (NO_3^-; α: 0.002, NO_2^- ; α: 0.4), and NO_2^- behaved non-conservatively in July 2016 (α: 0.6), indicating a possible loading event or production from possible sources such as groundwater, nitrogen fixation, nitrification, or denitrification. (Kendall, 1998). When separated into seasons, the NH_4^+, NO_2^-, and NO_3^- concentrations showed no statistically significant relationships with salinity except in the spring (March, April, May) when each of the components of DIN had a statistically significant relationship with salinity, consistent with mixing patterns (NH_4^+; R-squared: 0.4, α: 0.001, NO_2^-; R-squared: 0.5, α: 2.13e-05, and NO_3^- ; R-squared: 0.7, α: 1.8e-07). This is most likely due to riverine inputs and atmospheric deposition due to the rain events in the spring (Gardner et al., 2006; Seitzinger at al., 2002). Previous studies on both Baffin Bay and the surrounding area support this idea, as DIN concentrations remained relatively low throughout the study period unless punctuated by a rain or storm event (Wetz, 2017;

Mooney and McClelland, 2012). These results are consistent with the negative correlation between NO_2^- and salinity (Appendix H).

The NH_4^+ concentrations throughout the study period behaved conservatively with the salinity gradient in some months, and non-conservatively in others (Appendix C). A relatively strong conservative relationship between NH_4^+ concentrations and salinity were observed in the spring (R^2: 0.7, α: 0.001), followed by a weaker relationship in the fall (R^2: 0.2, α: 0.01). The conservative mixing relationship observed between NH_4^+ and the salinity gradient can be explained by the rainfall events in the spring, which would be a source of DIN to the water column via runoff. The non-conservative behavior of NH_4^+ in the summer and winter suggests the production or consumption of NH_4^+ rather than mixing alone. This is supported by the statistically significant (R^2: 0.1, α: 0.02) positive relationship between δ^{15}N-DIN and salinity [See Figure 13]**.** As NH_4^+ concentrations processed along the salinity gradient, the isotopic composition of the remaining NH_4^+ pool will be higher (Sigman et al., 2009; Denk, 2017).

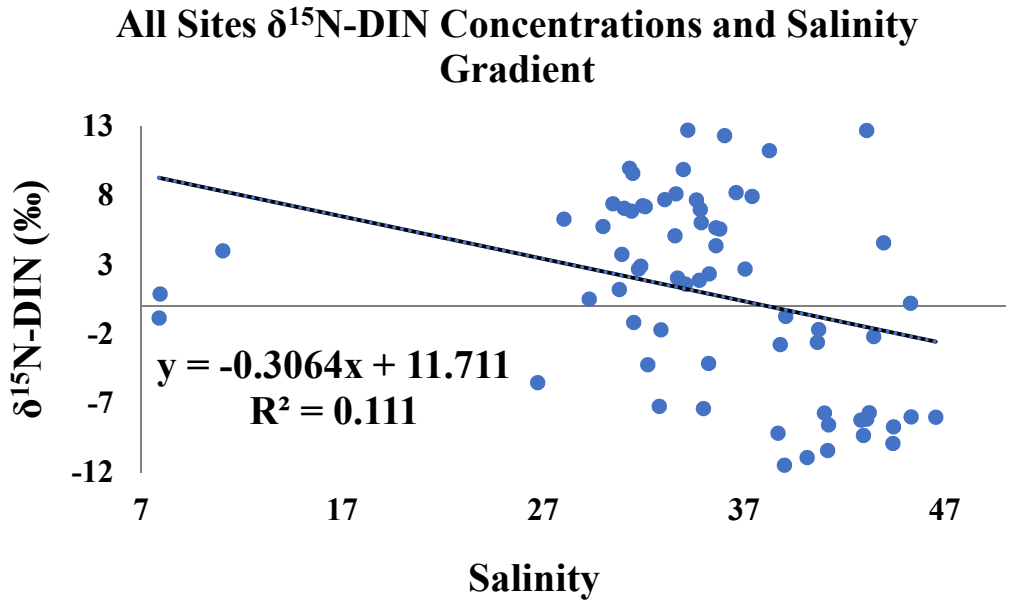

Figure 13. Figure of δ^{15}N-DIN values plotted against salinity showing relationship between δ^{15}N-DIN values and salinity. Trendline displays negative relationship (R^2: 0.1, α: 0.02) between δ^{15}N-DIN values and salinity.

Alternatively, during months that show non-conservative mixing patterns with the salinity gradient, it is possible that NH_4^+ is being produced. If a process such as photo-ammonification or remineralization is producing NH_4^+, the δ^{15}N-DIN of the produced NH_4^+ will be lower. This idea is supported by the positive correlation between NH_4^+ concentrations and δ^{15}N-DON values (r^2=0.80, α: 0.001) as this relationship can be attributed to internal N cycle processing mechanisms [See Figure 14](Appendix H). For example, the transformation of DON via photo-ammonification or mineralization, will result in an increase in NH_4^+ concentrations while leaving behind isotopically enriched δ^{15}N-DON (Denk, 2017; Sipler and Bronk, 2015; Morell & Corredor, 2001). This scenario is consistent with the previously discussed observation of isotopically low δ^{15}N-NH_4^+ in the summer indicating the production of isotopically light NH_4^+ via photo-ammonification, supported by the depletion of DON concentrations in August as well as a concurrent increase in the δ^{15}N-DON values [See Figure 14].

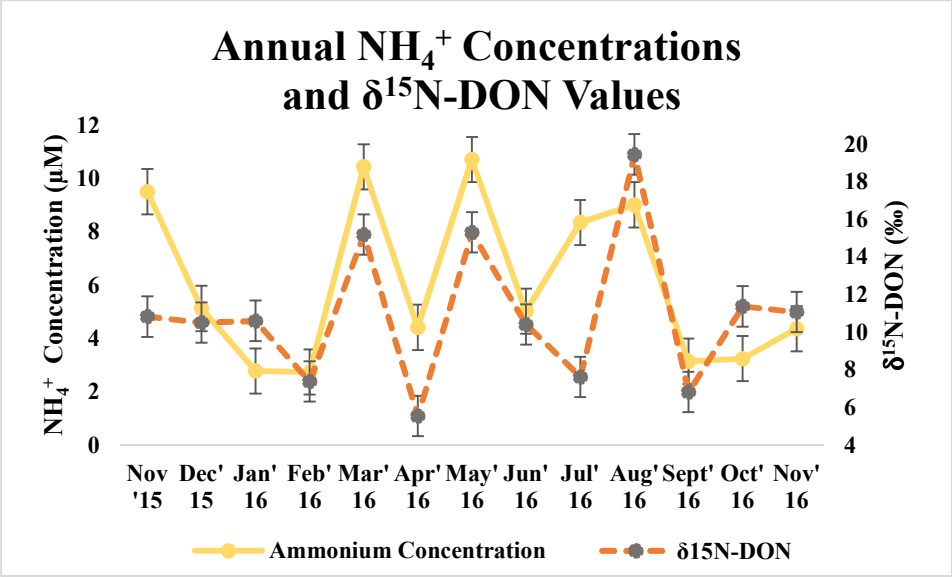

Figure 14. Figure of δ^{15}N-DON values plotted with NH_4^+ concentrations showing the relationship between annual δ^{15}N-DON values and NH_4^+ concentrations.

Seasonally, DON concentrations displayed conservative relationships with the salinity gradient in Baffin Bay in the spring and in the summer (Appendix C) [See Figure 15]. In May, the conservative relationship with salinity (R-squared: 0.65 α: 0.01), showed an increase of DON concentrations as the salinity increased. This mixing gradient could indicate possible in situ DON production rather than mixing from freshwater inputs or dilution of DON concentrations from the freshwater inputs and mixing of higher DON concentrations from the mouth of the bay. The in-situ production of DON is supported by the non-conservative relationship between δ^{15}N-DON and salinity indicating the involvement of a fractionating processing mechanism.

The non-conservative behavior of δ^{15}N-DON during May supports the involvement a fractionating process such as the consumption of DON from phytoplankton uptake as evidenced by the decrease of DON concentrations and increase of δ^{15}N-DON values in the spring. Additionally, this phytoplankton uptake and subsequent assimilation of NO_3^- and NH_4^+, which was loaded into the watershed by the rain events in the spring will eventually produce DON through

phytoplankton exudation, sloppy grazing or cell death (Sipler and Bronk, 2015; Wetz, 2015). This progression of the life cycle of phytoplankton is supported by the gradual increase of both DON concentrations and chlorophyll a from April to June.

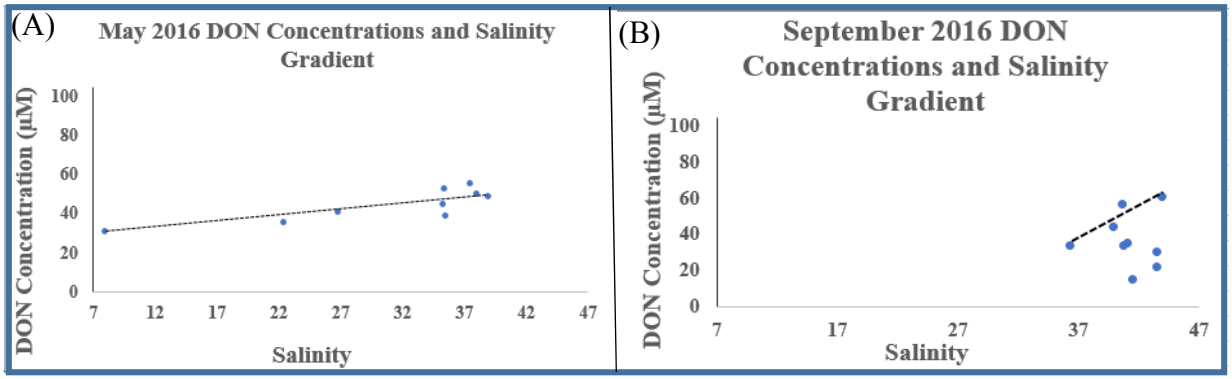

Figure 15. Panel A: Example of DON concentrations behaving conservatively with the salinity gradient in May 2016. Panel B: Example of DON concentrations behaving non-conservatively with the salinity gradient in September 2016.

The relationships observed between DON concentrations, δ^{15}N-DON and the salinity gradient confirm that internal processing of Nr is an important factor in the N-cycle at Baffin Bay. Schlarbuam et al., 2010 found similar results in the Elbe Estuary in northwest Europe as both DON and NH_4^+ concentrations were both consumed and produced as evidenced by non-conservative mixing gradients paired with dynamic isotope ratios along the salinity gradient (Schlarbaum et al., 2010). Further evidence for the role of fractionating processes and their effects on the δ^{15}N-DON values observed in Baffin Bay samples was evidenced by the results of the multivariate linear regression. The multivariate regression with δ^{15}N-DIN as the independent variable, with the previously listed explanatory variables yielded the following relationships:

Baffin Bay δ^{15}N-DON values= -0.13 DON concentration + 0.27 NH_4^+ concentration – 0.20 δ^{15}N-DIN values + 1.1 δ^{15}N-TDN values, $r^2 = 0.5179$

This regression indicates that δ^{15}N-DON values tend to increase when DON concentrations decrease. This is consistent with the effects associated with a fractionating process as DON is being broken down or consumed. Additionally, the δ^{15}N-DON values tend to increase with NH_4^+ concentrations and have an inverse relationship with δ^{15}N-DIN values. This also supports the predominance of fractionation from processing mechanisms, which will increase the δ^{15}N of the reactant (DON) as the reactant concentrations decrease and decrease the δ^{15}N of the product (NH_4^+) as the concentrations of the product increase. Additionally, the predominance of fractionation and internal processing in Baffin Bay is consistent with previous studies that have shown that systems with long residence times (Baffin Bay residence time >1 year) are more susceptible to various N- transformations within the system because of the prolonged retention of the nutrients, and lack of flushing (An and Gardner, 2002; Cloern, 2001; Pinckney et al., 2001.)

D. Crossplots of Nr concentration and isotopic composition

Previous studies have shown that the prominence of the processes of mixing and fractionation in watersheds can be differentiated using the linear relationship between the δ^{15}Nr and concentration of Nr (Burns et al., 2009, Kendall, 1998). For example, the mixing of two solutions with differing $\delta^{15}NH_4^+$ values and NH_4^+ concentrations are plotted, they are linear when isotope values are plotted as a function of 1/ [NH_4^+] (Burns et al., 2009; Kendall, 1998). However, fractionations occurring between differing biological N-processing mechanisms will show a linear relationship with NH_4^+ concentrations when the $\delta^{15}NH_4^+$ is plotted as a function of ln [NH_4^+] (Burns et al., 2009; Kendall, 1998). If no distinguishable linear relationship is observed, this suggests there is no single mixing or fractionating process that can be attributed to for the changes in isotopic values, but possibly multiple (Kendall, 1998, Zhang et al., 2014).

When looking at individual months throughout the study period, the only statistically significant relationship observed between δ^{15}N-DIN and DIN concentrations occurs in November 2015. In November 2015 the relationship between δ^{15}N-DIN and both 1/[DIN] and ln[DIN] showed evidence of mixing (α: 0.05) and a fractionating process (α: 0.01) [See Figure 16].

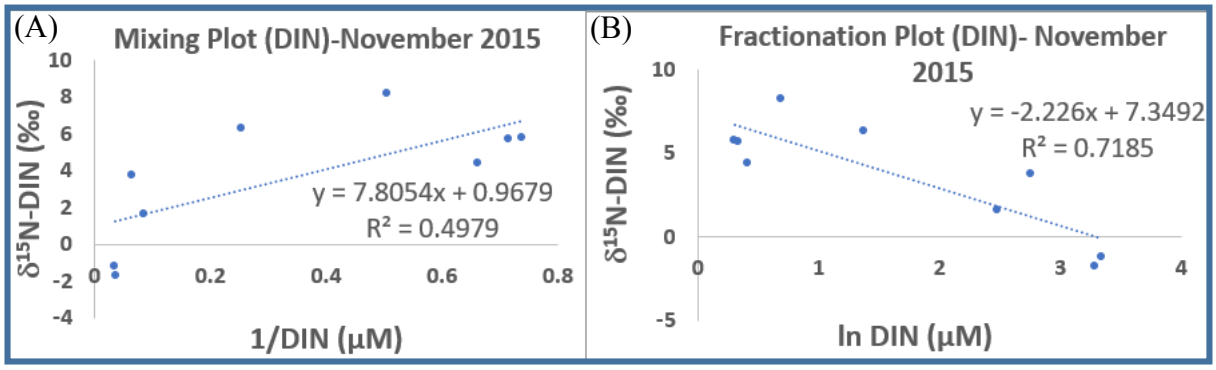

Figure 16. Panel of cross plots for DIN concentrations δ^{15}N-DIN values for November 2015. Panel A: δ^{15}N-DIN values are plotted as a function of 1/DIN. Panel B: δ^{15}N-DIN values are plotted as a function of ln(DIN).

When looking at the relationship of all sample DIN concentrations and δ^{15}N-DIN, a statistically significant linear relationship (R^2: 0.06, α: 0.05) is observed when δ^{15}N-DIN values are plotted against ln[DIN] [See Figure 17]. These results show that overall fractionating processes may play a larger role in the cycling of DIN in Baffin Bay when compared to mixing. This is consistent with the primarily non-conservative relationship of Nr concentrations with the salinity gradient.

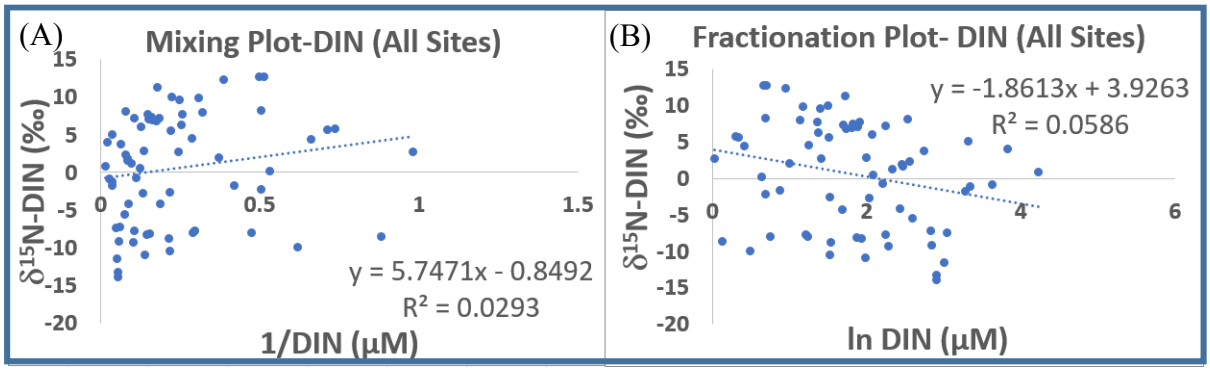

Figure 17. Panel of cross plots for DIN concentrations δ^{15}N-DIN values over all sites throughout the year. Panel A. δ^{15}N-DIN values are plotted as a function of 1/DIN. Panel B. δ^{15}N-DIN values are plotted as a function of ln(DIN).

Overall δ^{15}N-DON values throughout the year did not show a statistically significant relationship with ln[DON], but with 1/DON (r^2= 0.1, α: 0.05) which indicates that mixing may be the predominant factor dictating the variation in isotope values found throughout the year in Baffin Bay [See Figure 18]**.** However, when separated into seasons, δ^{15}N-DON showed statistically significant relationships with both 1/[DON] and ln[DON] (α: 0.02) during the summer, which implies that both mixing and fractionating processes may have been influencing the δ^{15}N-DON values at this time [See Figure 19].

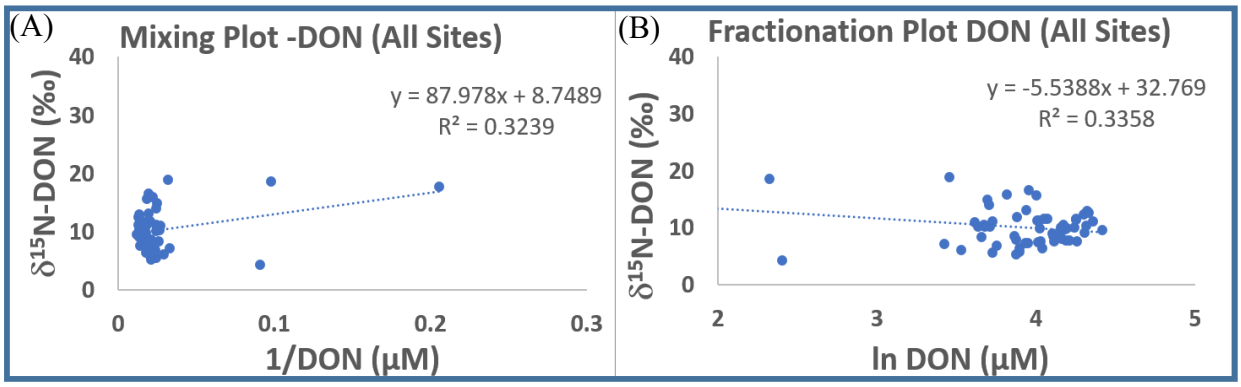

Figure 18. Panel of cross plots for DON concentrations δ^{15}N-DON values over all sites throughout the year. Panel A. δ^{15}N-DON values are plotted as a function of 1/DON. Panel B. δ^{15}N-DON values are plotted as a function of ln(DON).

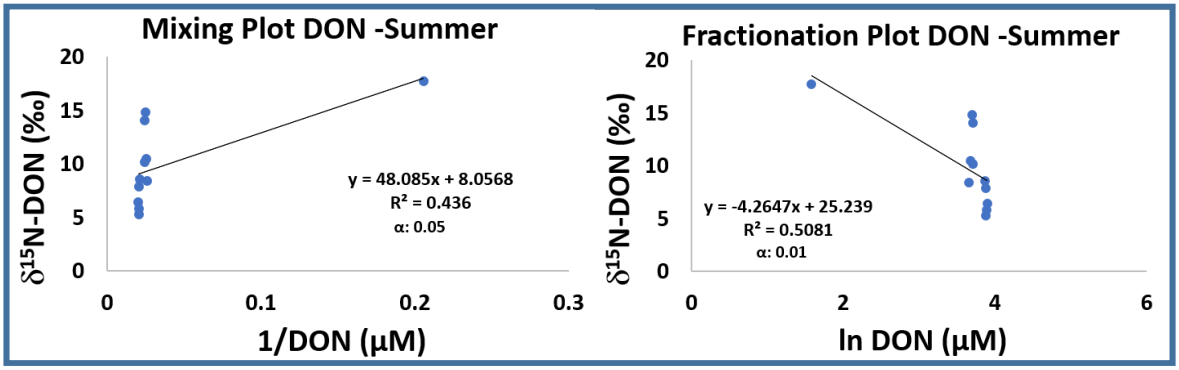

Figure 19. Cross plot of the relationship between δ^{15}N-DON and 1/DON and ln[DON] respectively in the summer.

The role of fractionating processes in cycling DON in Baffin Bay is further evidenced by the negative correlation between δ^{15}N-DON values and δ^{15}N-DIN values (α: 0.01) (Appendix H) which can be caused by various internal processing mechanisms such as mineralization, bacterial degradation, assimilation, and photo-ammonification**.** Each of these processes involves a reactant or product from the DIN pool to the DON pool or vice versa. The fractionation occurring during these processes is a possible explanation for negative correlation between δ^{15}N-DON values and

δ^{15}N-DIN values (Denk, 2017; Knapp et al., 2012; Kendall, 1998). For example, photo-ammonification is a process in which DON (the reactant) is degraded by UV exposure, and NH_4^+ (the product) is produced by this process and contributes to the DIN pool. The δ^{15}N-DON in the DON being degraded by the photo-ammonification process will become enriched in δ^{15}N as the lighter δ^{14}N is broken down more readily, and results in the production of NH_4^+ that has an isotopically low δ^{15}N-NH_4^+.

E. Photo-ammonification

Baffin Bay surface water samples collected in the spring and summer were exposed to photo-simulation in order to be able to compare seasonal differences in photo-ammonification rates. The summer water sample showed a gradual increase in NH_4^+ concentration concurrent with the increasing amount of time spent in the solar simulator [See Figure 20]. The overall concentration increased by approximately 20%. The results for the spring oxidation showed an initial decrease in NH_4^+ concentration, but a 4% increase was observed between hours 6 and 12 followed by a 20% increase between hours 12 and 24 [See Figure 21].

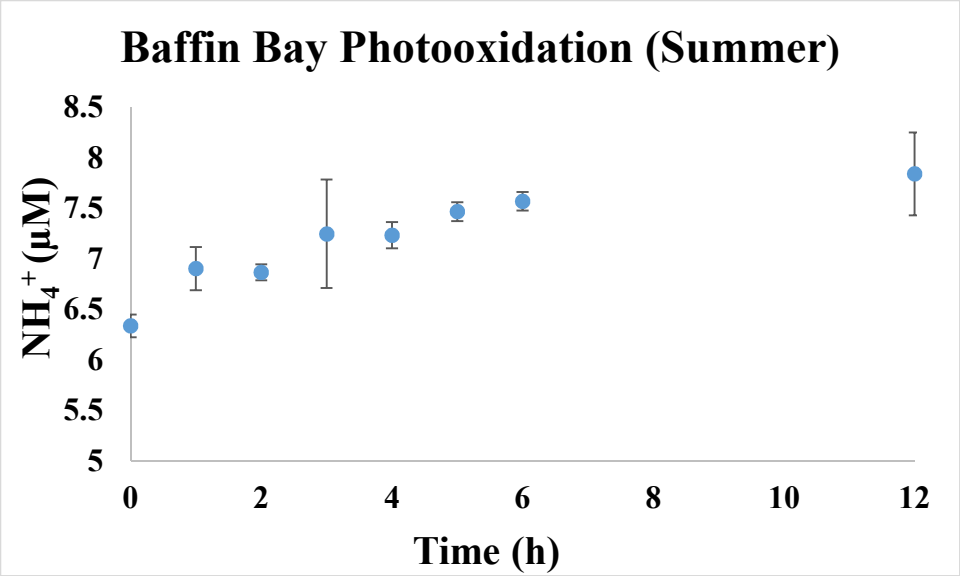

Figure 20. Results of the change in concentration of NH_4^+ of summer Baffin Bay samples exposed to a solar simulator UV lamp over 12-hour period.

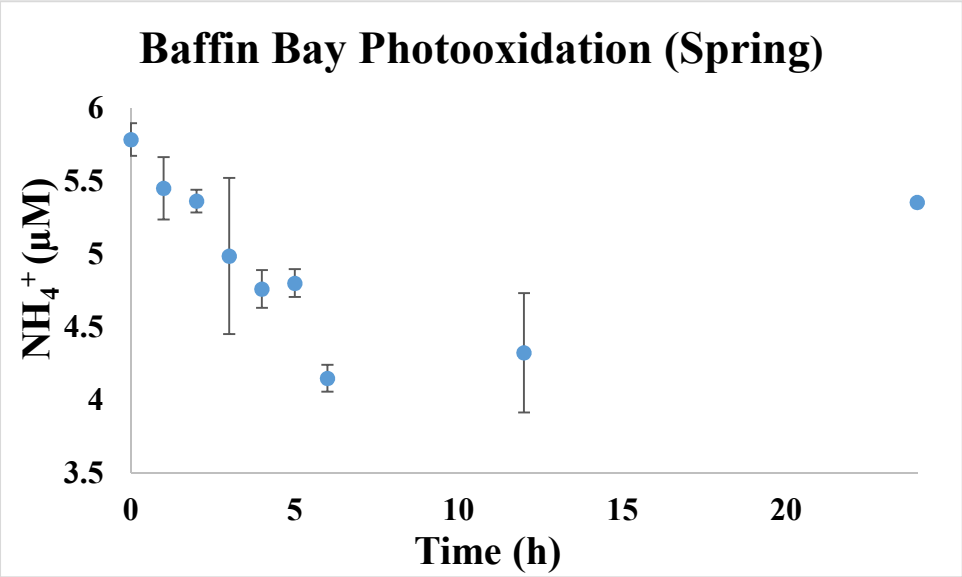

Figure 21. Results of the change in concentration of NH_4^+ of spring Baffin Bay samples exposed to a solar simulator UV lamp over 12-hour period.

The increase in NH_4^+ concentrations with continuous exposure to a UV lamp supports the theory that DON in Baffin Bay may be undergoing photodegradation and is contributing to the NH_4^+ pool (Bushaw et al., 1996; Shiller et al., 2006; Tarr et al., 2001). The importance of this

information was highlighted in a previous study regarding Swedish coastal waters, which demonstrated that additions of humic substances resulted in an increase in forms of available nitrogen and consequently increased levels of primary and secondary productivity (Bushaw et al., 1996). Another study conducted on the Orinco River in South America concluded that photomineralization of dissolved organic matter (DOM), and its release of NH_4^+ constitutes a significant source of bioavailable inorganic nitrogen that may be used to sustain phytoplankton biomass further down the river delta (Morell and Corredor, 2001). Photo-ammonification may play an important role in N-cycling in marine ecosystems similar to Baffin Bay where residence time is long and there is extended exposure to sunlight throughout the year. A recent study by Thibodeu et al., 2017, studied the isotope fractionation associated with DON removal in the Eurasian Arctic shelves and concluded that approximately 70% of total DON is either transformed by photo-ammonification or assimilated by bacterioplankton or phytoplankton (Thibodeaux et al., 2017). Additionally, when plotting the relationship between the δ^{15}N-DON values and ln(DON) concentrations for Baffin Bay during the summer, the calculated fractionation effect was approximately 4.3‰ which falls within the range of fractionation by photo-ammonification (~ 3‰ to 10 ‰) found in the Thibodeaux (2017) study. The effects of photo-ammonification and should be investigated further to determine the extent of its role in the N-cycle as well as it's fractionation effect on Nr.

CHAPTER IV- IMPLICATIONS AND CONCLUSIONS

In our study addressing both inorganic and organic nitrogen in Baffin Bay, we analyzed both the concentration and stable isotopic composition of N+N, DIN, and DON. Throughout the study period DON comprised ~90% of TDN, followed by NH_4^+ at ~8% on TDN and N+N at ~2% of

TDN. Seasonal variations of isotopic composition and concentrations were observed throughout the seasons due to multiple factors. The following seasonal stages summarize the main influences affecting $\delta^{15}N$ values throughout the study period [See Figure 22].

1. Elevated $\delta^{15}N$-DIN values (4.9‰ ± 5‰) in the winter indicate the influence of a source of DIN with a relatively high $\delta^{15}N$ such as wastewater or septic effluent, which may also contribute to elevated DON concentrations (46.4 μM ± 10 μM) and observed $\delta^{15}N$-DON values (9.5 ‰ ± 2 ‰).
2. The increase of NH_4^+ concentrations in the spring from run off caused by rain events concurrent with steady $\delta^{15}N$-DIN values (3.6‰ ± 6‰) implies that phytoplankton are using DON during this time as evidenced by high $\delta^{15}N$-DON values (12‰ ± 6‰) and relatively low DON concentrations (36 μM ± 13.2 μM).
3. Evidence of photo-ammonification is observed throughout the summer due to elevated $\delta^{15}N$-DON values (10.5‰ ± 3‰) and low ambient DON concentrations concurrent with low $\delta^{15}N$-DIN (-1‰ ± 5‰) and elevated NH_4^+ concentrations.
4. The accumulation of DON concentrations in the fall are consistent with phytoplankton detritus, which is supported by the decrease in $\delta^{15}N$-DON value averages in the fall and winter (9.8‰ ± 2‰). Remineralization during this stage is supported by low $\delta^{15}N$-DIN values (-2.3‰ ± 4.4‰).

The relatively high $\delta^{15}N$-DIN values (4.9‰ ± 5‰) observed during the winter in Stage 1 could be attributed to a source with a higher $\delta^{15}N$ signature such as wastewater or septic effluent (+10 to +25‰). The contribution of sources of Nr to Baffin Bay is dependent on hydrological conditions, and it has been observed that the riverine tributaries that feed into the branches of Baffin Bay can become stagnant during dry conditions or droughts. It during these dry months that more consistent

flows such as wastewater effluent or septic systems may have a greater contribution on Nr inputs and $\delta^{15}N$ values than other external inputs of Nr such as runoff, atmospheric deposition, and riverine inputs. Additionally, a review conducted by Pehlivanoglu-Mantas and Sedlak stated that the removal of organic nitrogen from wastewater treatment plants is often inefficient, and DON can comprise up to 65% of the dissolved nitrogen in these effluents (Pehlivanoglu-Mantas and Sedlak, 2006). This is supported by elevated DON concentrations (46 μM ± 10 μM) and $\delta^{15}N$-DON values (9.5‰ ± 2‰) observed during the winter months.

The increase of NH_4^+ concentrations from increased run off caused by spring rain events is evidenced by conservative mixing relationships with the salinity gradient concurrent with rain events as well as $\delta^{15}N$-N+N values in the spring months ($\delta^{15}N$-N+N: 5.6‰ ± 3‰, O^{18}: 10.8 ‰ ± 2.1‰) consistent with the influence of atmospheric depositions ($\delta^{15}N$-NO_3^-: -15‰ to +15‰ and $\delta^{18}O$: +65‰ to +95‰) as well as synthetic fertilizers ($\delta^{15}N$-NO_3^-: −5 to +8‰ and $\delta^{18}O$: +15 to +25‰), which would be introduced into the watershed via run-off. The increase of NH_4^+ concentrations and consistent $\delta^{15}N$-DIN values in Stage 2 during the spring (4.9‰ ± 4.3‰) implies that phytoplankton are using bioavailable DON during this time. This scenario is supported by the elevated $\delta^{15}N$-DON values (12‰ ± 6‰) and low DON concentrations (40 μM ± 13 μM) throughout the spring months.

In the summer a decrease in DON concentration is observed in Stage 3 with high $\delta^{15}N$-DON values (12.5‰ ± 6‰), likely attributed to photo-ammonification from the increased exposure of DON to UV radiation. This processing mechanism is supported by relatively elevated NH_4^+ concentrations with low $\delta^{15}N$-DIN values (-1.6‰ ± 4‰) in the summer.

DON can be released by the process of viral lysis or cell death of bacteria and phytoplankton (Berman and Bronk, 2003). The elevated DON concentrations (58 μM ± 13 μM) in the fall

observed in Stage 4 are consistent with phytoplankton detritus and the associated exudation of DON towards the end of their growth cycle (Biddanda and Benner, 1997). This is also supported by the decrease in average chlorophyll a levels observed in the fall and winter. Additional evidence for phytoplankton die off is observed with the decrease of the δ^{15}N-DON values in the fall and winter. The exudation of extracellular products in the form of DON after cell death would be depleted in ^{15}N relative to the δ^{15}N of the phytoplankton (Checkley Jr and Miller, 1989). Additionally, bacterial degradation of the available DON after the phytoplankton biomass die off would contribute to the lower δ^{15}N-DIN values observed in the fall.

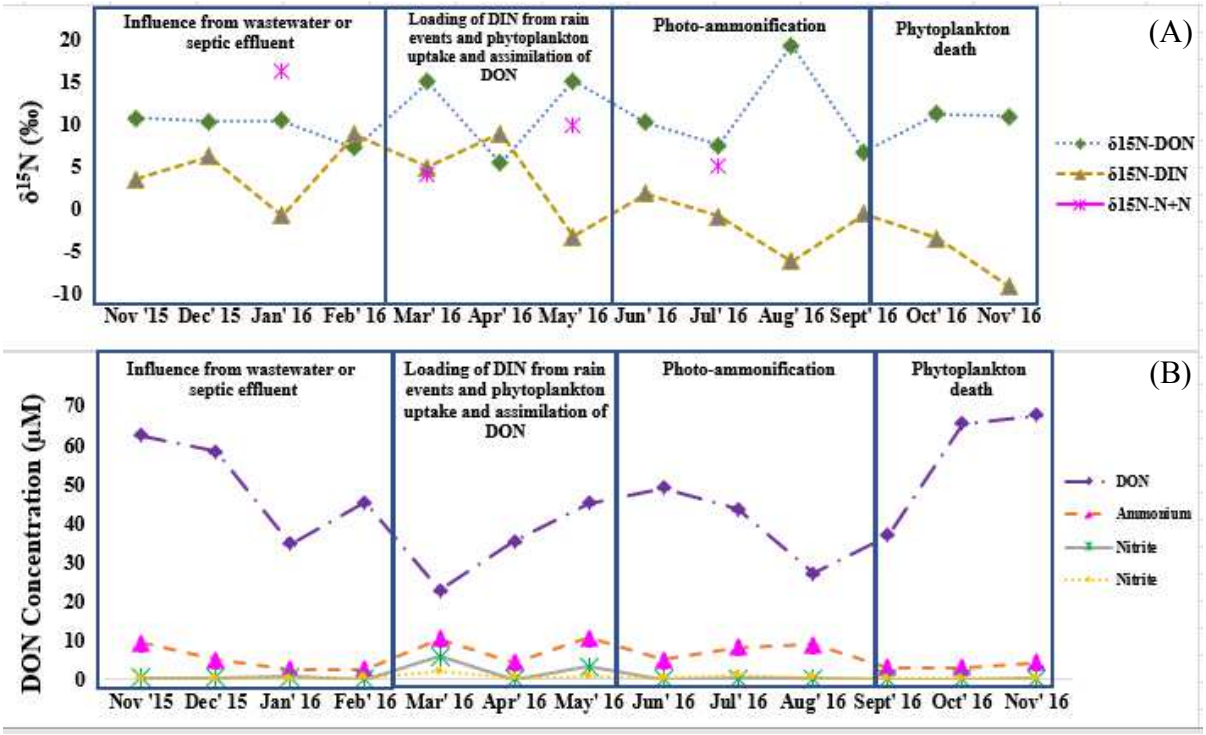

Figure 22. δ^{15}N and Nr concentration times series for Baffin Bay sites throughout the study period. Panel A includes δ^{15}N of DIN, DON, and N+N throughout the study period. Panel B includes the concentrations of DON, NH_4^+, NO_3^-, and NO_2^- throughout the study period.

Salinity gradients and cross plots of the relationships between Nr concentrations and δ^{15}Nr values both support the idea that while both mixing and processing can be affect δ^{15}N values throughout the year, Nr processing (i.e. photo-ammonification, phytoplankton uptake, bacterial mineralization) may be the dominant mechanism for N cycling in Baffin Bay. This idea is consistent with previous studies that have shown that systems with long residence times, such as Baffin Bay (>1 year) are more susceptible to various N- transformations within the system because of the prolonged retention of the nutrients, and lack of flushing. The results of this project, as well as the experimental methodology, can be useful and applicable to estuarine ecosystems in various settings, advancing scientific progress towards mitigating blooms. Additionally, since the elevated concentrations of DON make Baffin Bay uniquely suited to investigate its sources and processing, this project aids in characterizing the role of this largely unstudied form of Nr, provides insights to the role of DON in nitrogen dynamics.

REFERENCES

Alkhatib, M., Lehmann, M.F., Del Giorgio, P.A., 2012. The nitrogen isotope effect of benthic remineralization-nitrification-denitrification coupling in an estuarine environment. Biogeosciences 9, 1633–1646.

Aluwihare, L.I., Repeta, D.J., Pantoja, S., Johnson, C.G., 2005. Two Chemically Distinct Pools of Organic Nitrogen Accumulate in the Ocean. Science 308, 1007–1010. https://doi.org/10.1126/science.1108925

American Society for Testing and Materials. 1993. Std. Methods 4500-NO3 F (21st edition) EPA 353.2 version 2 (1993) In Annual book of ASTM standards, section 11, water and environmental technology, vol. 11.02. Water (II). American Society for Testing and Materials, Philadelphia.

An, S., Gardner, W.S., 2002. Dissimilatory nitrate reduction to ammonium (DNRA) as a nitrogen link, versus denitrification as a sink in a shallow estuary (Laguna Madre/Baffin Bay, Texas). Marine Ecology Progress Series 237, 41–50.

Avery, G.B., Foley, L., Carroll, A.L., Roebuck, J.A., Guy, A., Mead, R.N., Kieber, R.J., Willey, J.D., Skrabal, S.A., Felix, J.D., Mullaugh, K.M., Helms, J.R., 2016. Surface waters as a sink and source of atmospheric gas phase ethanol. Chemosphere 144, 360–365. https://doi.org/10.1016/j.chemosphere.2015.08.080

Badr, E.-S.A., Tappin, A.D., Achterberg, E.P., 2008. Distributions and seasonal variability of dissolved organic nitrogen in two estuaries in SW England. Marine Chemistry 110, 153–164. doi:10.1016/j.marchem.2008.04.007

Berman, T., Bronk, D.A., 2003. Dissolved organic nitrogen: a dynamic participant in aquatic ecosystems. AquatMicrobEcol 31, 279–305. doi:10.3354/ame031279

Biddanda, B., Benner, R., 1997. Carbon, nitrogen, and carbohydrate fluxes during the production of particulate and dissolved organic matter by marine phytoplankton. Limnology and Oceanography 42, 506–518.

Burns, D.A., Boyer, E.W., Elliott, E.M., Kendall, C., 2009. Sources and transformations of nitrate from streams draining varying land uses: evidence from dual isotope analysis. J. Environ. Qual. 38, 1149–1159. https://doi.org/10.2134/jeq2008.0371

Bushaw, K.L., Zepp, R.G., Tarr, M.A., al, et, 1996. Photochemical release of biologically available nitrogen from aquatic dissolved organic matter. Nature; London 381, 404.

Buskey, E.J., Montagna, P.A., Amos, A.F., Whitledge, T.E., 1997. Disruption of Grazer Populations as a Contributing Factor to the Initiation of the Texas Brown Tide Algal Bloom. Limnology and Oceanography 42, 1215–1222.

Buskey, E.J., Liu, H., Collumb, C., Bersano, J.G.F., 2001. The decline and recovery of a persistent Texas brown tide algal bloom in the Laguna Madre (Texas, USA). Estuaries 24, 337–346. doi:10.2307/1353236

Bronk, D.A., See, J.H., Bradley, P., Killberg, L., 2007. DON as a source of bioavailable nitrogen for phytoplankton. Biogeosciences 4, 283–296.

Bronk, D.A., Lomas, M.W., Glibert, P.M., Schukert, K.J., Sanderson, M.P., 2000. Total dissolved nitrogen analysis: comparisons between the persulfate, UV and high temperature oxidation methods. Marine Chemistry 69, 163–178. doi:10.1016/S0304-4203(99)00103-6

Bricelj, V. Monica, and Darcy J. Lonsdale. “Aureococcus Anophagefferens: Causes and Ecological Consequences of Brown Tides in U.S. Mid-Atlantic Coastal Waters.”

Limnology and Oceanography 42, no. 5part2 (July 1, 1997): 1023–38. doi:10.4319/lo.1997.42.5_part_2.1023.

Casciotti, K.L., 2016. Nitrite isotopes as tracers of marine N cycle processes. Phil. Trans. R. Soc. A 374, 20150295. https://doi.org/10.1098/rsta.2015.0295

Collos, Y., 1998. Nitrate uptake, nitrite release and uptake, and new production estimates. Marine Ecology Progress Series 293–301.

Chisholm, S.W., 1992. Phytoplankton size, in: Primary Productivity and Biogeochemical Cycles in the Sea. Springer, pp. 213–237.

Checkley Jr, D.M., Miller, C.A., 1989. Nitrogen isotope fractionation by oceanic zooplankton. Deep Sea Research Part A. Oceanographic Research Papers 36, 1449–1456.

Choi, W.-J., Kwak, J.-H., Lim, S.-S., Park, H.-J., Chang, S.X., Lee, S.-M., Arshad, M.A., Yun, S.-I., Kim, H.-Y., 2017. Synthetic fertilizer and livestock manure differently affect $\delta^{15}N$ in the agricultural landscape: A review. Agriculture, ecosystems & environment 237, 1–15.

Cloern, J.E., 2001. Our evolving conceptual model of the coastal eutrophication problem. Marine ecology progress series 210, 223–253.

Denk, T.R.A., Mohn, J., Decock, C., Lewicka-Szczebak, D., Harris, E., Butterbach-Bahl, K., Kiese, R., Wolf, B., 2017. The nitrogen cycle: A review of isotope effects and isotope modeling approaches. Soil Biology and Biochemistry 105, 121–137. doi:10.1016/j.soilbio.2016.11.015

DeYoe, H.R., Suttle, C.A., 1994. The Inability of the Texas "Brown Tide" Alga to Use Nitrate and the Role of Nitrogen in the Initiation of a Persistent Bloom of This

Organism1. Journal of Phycology 30, 800–806. doi:10.1111/j.0022-3646.1994.00800.x

David Felix, J., Elliott, E.M., Gish, T.J., McConnell, L.L., Shaw, S.L., 2013. Characterizing the isotopic composition of atmospheric ammonia emission sources using passive samplers and a combined oxidation-bacterial denitrifier approach. Rapid Commun. Mass Spectrom. 27, 2239–2246. doi:10.1002/rcm.6679

Eaton, A.D., American Public Health Association, American Water Works Association, Water Environment Federation, 2005. Standard methods for the examination of water and wastewater. APHA-AWWA-WEF, Washington, D.C.

French, D.P., Furnas, M.J., Smayda, T.J., 1983. Diel changes in nitrite concentration in the chlorophyll maximum in the Gulf of Mexico. Deep Sea Research Part A. Oceanographic Research Papers 30, 707–722.

Fry, B., Parker, P.L., 1979. Animal diet in Texas seagrass meadows: δ13C evidence for the importance of benthic plants. Estuarine and Coastal Marine Science 8, 499–509. doi:10.1016/0302-3524(79)90031-8

Gardner, W.S., McCarthy, M.J., An, S., Sobolev, D., Sell, K.S., Brock, D., 2006. Nitrogen fixation and dissimilatory nitrate reduction to ammonium (DNRA) support nitrogen dynamics in Texas estuaries. Limnology and Oceanography 51, 558–568.

Gasol, J.M., del Giorgio, P.A., Massana, R., Duarte, C.M., 1995. Active versus inactive bacteria: size-dependence in a coastal marine plankton community. Marine Ecology Progress Series 91–97.

Glibert, P.M., Wazniak, C.E., Hall, M.R., Sturgis, B., 2007. Seasonal and interannual trends in nitrogen and brown tide in Maryland's coastal bays. Ecological Applications 17.

Gobler, C.J., Renaghan, M.J., Buck, N.J., 2002. Impacts of Nutrients and Grazing Mortality on the Abundance of Aureococcus anophagefferens during a New York Brown Tide Bloom. Limnology and Oceanography 47, 129–141.

Gobler, Christopher J., and William G. Sunda. "Ecosystem Disruptive Algal Blooms of the Brown Tide Species, Aureococcus anophagefferens and Aureoumbra lagunensis." Harmful Algae, Harmful Algae--The requirement for species-specific information, 14 (February 2012): 36–45. doi:10.1016/j.hal.2011.10.013.

Granger, J., Sigman, D.M., Needoba, J.A., Harrison, P.J., 2004. Coupled nitrogen and oxygen isotope fractionation of nitrate during assimilation by cultures of marine phytoplankton. Limnology and Oceanography 49, 1763–1773.

Hadas, O., M. A. Altabet, and R. Agnihotri. "Seasonally Varying Nitrogen Isotope Biogeochemistry of Particulate Organic Matter in Lake Kinneret, Israel," 2009. http://drs.nio.org/drs/handle/2264/2596.

Hastings, M.G., Steig, E.J., Sigman, D.M., n.d. Seasonal variations in N and O isotopes of nitrate in snow at Summit, Greenland: Implications for the study of nitrate in snow and ice cores. Journal of Geophysical Research: Atmospheres 109. https://doi.org/10.1029/2004JD004991

Heaton, T. H. E. "Isotopic Studies of Nitrogen Pollution in the Hydrosphere and Atmosphere: A Review." *Chemical Geology: Isotope Geoscience Section*, Calibration

of the Phanerozoic Time Scale, 59 (January 1, 1986): 87–102. doi:10.1016/0168-9622(86)90059-X.

Hoagland, P., and S. Scatasta. "The Economic Effects of Harmful Algal Blooms." In Ecology of Harmful Algae, edited by Prof Dr. Edna Granéli and Prof Dr. Jefferson T. Turner, 391–402. Ecological Studies 189. Springer Berlin Heidelberg, 2006. http://link.springer.com/chapter/10.1007/978-3-540-32210-8_30.

Holmes, R.M., Aminot, A., Kérouel, R., Hooker, B.A., Peterson, B.J., 1999. A simple and precise method for measuring ammonium in marine and freshwater ecosystems. Can. J. Fish. Aquat. Sci. 56, 1801–1808. https://doi.org/10.1139/f99-128

Kelly, J.R., 2008. Nitrogen effects on coastal marine ecosystems, in: Nitrogen in the Environment (Second Edition). Elsevier, pp. 271–332.

Kendall, C., Caldwell, E.A., 1998. Fundamentals of isotope geochemistry. Isotope tracers in catchment hydrology 51–86.

Kendall, C., Elliott, E.M., Wankel, S.D., 2007. Tracing anthropogenic inputs of nitrogen to ecosystems. Stable isotopes in ecology and environmental science 2, 375–449.

Kessel, C. van, Farrell, R.E., Pennock, D.J., 1994. Carbon-13 and nitrogen-15 natural abundance in crop residues and soil organic matter. Soil Science Society of America journal (USA).

Knapp, A.N., Sigman, D.M., Kustka, A.B., Sañudo-Wilhelmy, S.A., Capone, D.G., 2012. The distinct nitrogen isotopic compositions of low and high molecular weight marine DON. Marine Chemistry 136, 24–33.

Knapp, A.N., Sigman, D.M., Lipschultz, F., 2005. N isotopic composition of dissolved organic nitrogen and nitrate at the Bermuda Atlantic Time-series Study site. Global Biogeochemical Cycles 19.

Lee, K.-S., Lee, D.-S., Lim, S.-S., Kwak, J.-H., Jeon, B.-J., Lee, S.-I., Lee, S.-M., Choi, W.-J., 2012. Nitrogen isotope ratios of dissolved organic nitrogen in wet precipitation in a metropolis surrounded by agricultural areas in southern Korea. Agriculture, Ecosystems & Environment 159, 161–169. https://doi.org/10.1016/j.agee.2012.07.010

Lehmann, M.F., Sigman, D.M., Berelson, W.M., 2004. Coupling the 15N/14N and 18O/16O of nitrate as a constraint on benthic nitrogen cycling. Marine Chemistry 88, 1–20.

Lomas, M.W., Kana, T.M., MacIntyre, H.L., Cornwell, J.C., Nuzzi, R., Waters, R., 2004. Interannual variability of Aureococcus anophagefferens in Quantuck Bay, Long Island: natural test of the DON hypothesis. Harmful Algae 3, 389–402.

Lomas, M.W., Lipschultz, F., 2006. Forming the primary nitrite maximum: Nitrifiers or phytoplankton? Limnology and Oceanography 51, 2453–2467.

Mooney, R.F., McClelland, J.W., 2012. Watershed export events and ecosystem responses in the Mission–Aransas National Estuarine Research Reserve, south Texas. Estuaries and coasts 35, 1468–1485.

Morell, J.M., Corredor, J.E., 2001. Photomineralization of fluorescent dissolved organic matter in the Orinoco River plume: Estimation of ammonium release. J. Geophys. Res. 106, 16807–16813. doi:10.1029/1999JC000268

Nestler, A., Berglund, M., Accoe, F., Duta, S., Xue, D., Boeckx, P., Taylor, P., 2011. Isotopes for improved management of nitrate pollution in aqueous resources: review of

surface water field studies. Environ Sci Pollut Res 18, 519–533. https://doi.org/10.1007/s11356-010-0422-z

Ockerman, D.J., Petri, B.L., Texas Agricultural Experiment Station, Caesar Kleberg Wildlife Research Institute, Coastal Bend Bays & Estuaries Program, Geological Survey (U.S.), 2001. Hydrologic conditions and water quality in an agricultural area in Kleberg and Nueces counties, Texas, 1996-98. U.S. Dept. of the Interior, U.S. Geological Survey, Austin, Tex.

Ogawa & Co., NO, NO2, NOx and SO2 sampling protocol using the ogawa sampler. 1998. Accessed at www.agawausa.com in 2016.

Onuf, C.P. "Seagrass Responses to Long-Term Light Reduction by Brown Tide in Upper Laguna Madre, Texas: Distribution and Biomass Patterns." *Marine Ecology Progress Series* 138 (July 25, 1996): 219–31. doi:10.3354/meps138219.

Paerl, H.W., Dennis, R.L., Whitall, D.R., 2002. Atmospheric deposition of nitrogen: implications for nutrient over-enrichment of coastal waters. Estuaries 25, 677–693.

Paerl, H.W., Gardner, W.S., Havens, K.E., Joyner, A.R., McCarthy, M.J., Newell, S.E., Qin, B., Scott, J.T., 2016. Mitigating cyanobacterial harmful algal blooms in aquatic ecosystems impacted by climate change and anthropogenic nutrients. Harmful Algae 54, 213–222.

Pehlivanoglu-Mantas, E., Sedlak, D.L., 2006. Wastewater-derived dissolved organic nitrogen: analytical methods, characterization, and effects—a review. Critical Reviews in Environmental Science and Technology 36, 261–285.

Pennock, J.R., Boyer, J.N., Herrera-Silveira, J.A., Iverson, R.L., Whitledge, T.E., Mortazavi, B., Comin, F.A., 1999. Nutrient behavior and phytoplankton production

in Gulf of Mexico estuaries. Biogeochemistry of Gulf of Mexico Estuaries. John Wiley & Sons 109–162.

Pennock, J.R., Velinsky, D.J., Ludlam, J.M., Sharp, J.H., Fogel, M.L., 1996. Isotopic Fractionation of Ammonium and Nitrate During Uptake by Skeletonemacostatum: Implications for $\delta^{15}N$ Dynamics Under Bloom Conditions. Limnology and Oceanography 41, 451–459.

Peterson, B.J. and Fry, B. "Stable Isotopes in Ecosystem Studies." *Annual Review of Ecology and Systematics* 18, no. 1 (1987): 293–320. doi:10.1146/annurev.es.18.110187.001453.

Pinckney, J.L., Paerl, H.W., Tester, P., Richardson, T.L., 2001. The role of nutrient loading and eutrophication in estuarine ecology. Environmental Health Perspectives 109, 699.

Rennie, D.A., Paul, E.A., Johns, L.E., 1976. Natural nitrogen-15 abundance of soil and plant samples. Canadian Journal of Soil Science 56, 43–50.

Robertson, B.R., Button, D.K., n.d. Characterizing aquatic bacteria according to population, cell size, and apparent DNA content by flow cytometry. Cytometry 10, 70–76. https://doi.org/10.1002/cyto.990100112

Santos, I.R., Burnett, W.C., Dittmar, T., Suryaputra, I.G., Chanton, J., 2009. Tidal pumping drives nutrient and dissolved organic matter dynamics in a Gulf of Mexico subterranean estuary. Geochimica et Cosmochimica Acta 73, 1325–1339.

Schlarbaum, T., Daehnke, K., Emeis, K., 2010. Turnover of combined dissolved organic nitrogen and ammonium in the Elbe estuary/NW Europe: Results of nitrogen isotope investigations. Marine Chemistry 119, 91–107. doi:10.1016/j.marchem.2009.12.007

Seitzinger, S.P., Sanders, R.W., 1999. Atmospheric inputs of dissolved organic nitrogen stimulate estuarine bacteria and phytoplankton. Limnol. Oceanogr. 44, 721–730. doi:10.4319/lo.1999.44.3.0721

Seitzinger, S.P., Sanders, R.W., Styles, R., 2002. Bioavailability of DON from natural and anthropogenic sources to estuarine plankton. Limnol. Oceanogr. 47, 353–366. doi:10.4319/lo.2002.47.2.0353

Semi, D.O.A.N.B., 1993. Method 350.1 Determination of Ammonia Nitrogen by Semi-Automated Colorimetry.

Shiller, A.M., Duan, S., van Erp, P., Bianchi, T.S., 2006. Photo-oxidation of dissolved organic matter in river water and its effect on trace element speciation. Limnology and Oceanography 51, 1716–1728.

Sigman, D. M., K. L. Karsh, and K. L. Casciotti. "Ocean process tracers: nitrogen isotopes in the ocean." *Encyclopedia of ocean science, 2nd edn Elsevier, Amsterdam* (2009).

Silva, S.R., Ging, P.B., Lee, R.W., Ebbert, J.C., Tesoriero, A.J., Inkpen, E.L., 2002. Forensic applications of nitrogen and oxygen isotopes in tracing nitrate sources in urban environments. Environmental Forensics 3, 125–130.

Simms, A.R., Aryal, N., Miller, L., Yokoyama, Y., 2010. The incised valley of Baffin Bay, Texas: a tale of two climates. Sedimentology 57, 642–669. doi:10.1111/j.1365-3091.2009.01111.x

Singleton, M.J., Esser, B.K., Moran, J.E., Hudson, G.B., McNab, W.W., Harter, T., 2007. Saturated Zone Denitrification: Potential for Natural Attenuation of Nitrate Contamination in Shallow Groundwater Under Dairy Operations. Environ. Sci. Technol. 41, 759–765. https://doi.org/10.1021/es061253gSmith, N.P., 1977.

Meteorological and tidal exchanges between Corpus Christi Bay, Texas, and the northwestern Gulf of Mexico. Estuarine and Coastal Marine Science 5, 511–520. doi:10.1016/0302-3524(77)90098-6

Sipler, R.E., Bronk, D.A., 2014. Dynamics of dissolved organic nitrogen, in: Biogeochemistry of Marine Dissolved Organic Matter (Second Edition). Elsevier, pp. 127–232.

Tarr, M.A., Wang, W., Bianchi, T.S., Engelhaupt, E., 2001. Mechanisms of ammonia and amino acid photoproduction from aquatic humic and colloidal matter. Water Research 35, 3688–3696.

Thibodeau, B., Bauch, D., Voss, M., 2017. Nitrogen dynamic in Eurasian coastal Arctic ecosystem: Insight from nitrogen isotope. Global Biogeochemical Cycles 31, 836–849.

Tsunogai, U., Kido, T., Hirota, A., Ohkubo, S. B., Komatsu, D. D. and Nakagawa, F. (2008), Sensitive determinations of stable nitrogen isotopic composition of organic nitrogen through chemical conversion into N_2O. Rapid Commun. Mass Spectrom., 22: 345–354. doi: 10.1002/rcm.3368

Turner, R.E., Qureshi, N., Rabalais, N.N., Dortch, Q., Justic, D., Shaw, R.F., Cope, J., 1998. Fluctuating silicate: nitrate ratios and coastal plankton food webs. Proceedings of the National Academy of Sciences 95, 13048–13051.

Umezawa, Y., Hosono, T., Onodera, S., Siringan, F., Buapeng, S., Delinom, R., Yoshimizu, C., Tayasu, I., Nagata, T., Taniguchi, M., 2008. Sources of nitrate and ammonium contamination in groundwater under developing Asian megacities. Science of The Total Environment, BIOGEOCHEMISTRY OF FORESTED ECOSYSTEM - Selected papers from BIOGEOMON, the 5th International Symposium on Ecosystem

Behaviour, held at the University of California, Santa Cruz, on June 25–30, 2006 404, 361–376. https://doi.org/10.1016/j.scitotenv.2008.04.021

Viana, I.G., Bode, A., 2015. Variability in $\delta^{15}N$ of intertidal brown algae along a salinity gradient: Differential impact of nitrogen sources. Science of the Total Environment 512, 167–176.

Wankel, S.D., Kendall, C., Paytan, A., 2009. Using nitrate dual isotopic composition (δ15N and δ18O) as a tool for exploring sources and cycling of nitrate in an estuarine system: Elkhorn Slough, California. Journal of Geophysical Research: Biogeosciences 114.

Wankel, S.D., Kendall, C., Francis, C.A., Paytan, A., n.d. Nitrogen sources and cycling in the San Francisco Bay Estuary: A nitrate dual isotopic composition approach. Limnology and Oceanography 51, 1654–1664. https://doi.org/10.4319/lo.2006.51.4.1654

Waycott, M., Duarte, C.M., Carruthers, T.J., Orth, R.J., Dennison, W.C., Olyarnik, S., Calladine, A., Fourqurean, J.W., Heck, K.L., Hughes, A.R., others, 2009. Accelerating loss of seagrasses across the globe threatens coastal ecosystems. Proceedings of the National Academy of Sciences 106, 12377–12381.

Wetz, M.S., Cira, E.K., Sterba-Boatwright, B., Montagna, P.A., Palmer, T.A., Hayes, K.C., Exceptionally high organic nitrogen concentrations in a semi-arid south Texas estuary susceptible to brown tide blooms, Estuarine, Coastal and Shelf Science (2017), doi: 10.1016/ j.ecss.2017.02.001.

Wetz, M.S., 2015. Baffin Bay Volunteer Water Quality Monitoring Study: Synthesis of May 2013-July 2015 Data. Synthesis.

Zhang, L., Altabet, M.A., Wu, T., Hadas, O., 2007. Sensitive measurement of NH_4^+ 15N/14N ($\delta^{15}NH_4^+$) at natural abundance levels in fresh and saltwaters. Analytical Chemistry 79, 5297–5303.

Zhang, Y., Li, F., Zhang, Q., Li, J., Liu, Q., 2014. Tracing nitrate pollution sources and transformation in surface-and ground-waters using environmental isotopes. Science of the Total Environment 490, 213–222.

LIST OF APPENDICES

APPENDIX PAGE

Appendix A

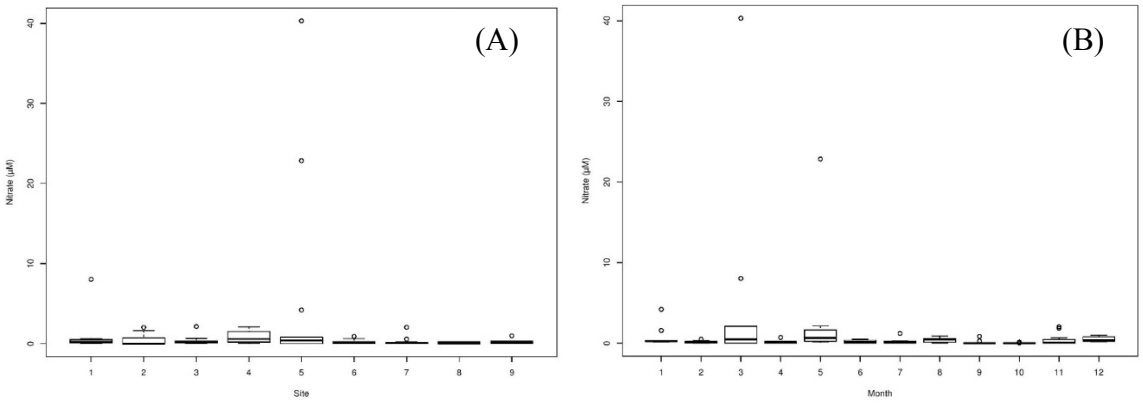

Figure A.1: Panel A shows box plot of NO_3^- concentrations by site and Panel B shows box plots of NO_3^- concentrations by month.

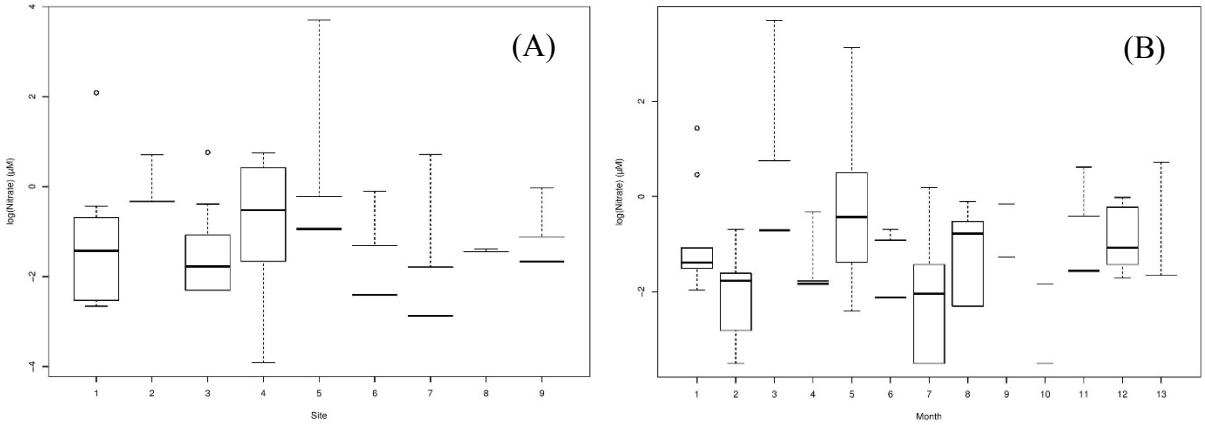

Figure A.2: Panel A shows boxplot of log(NO_3^-) concentrations by site and Panel B shows box plots of log (NO_3^-) concentrations by month.

Appendix B

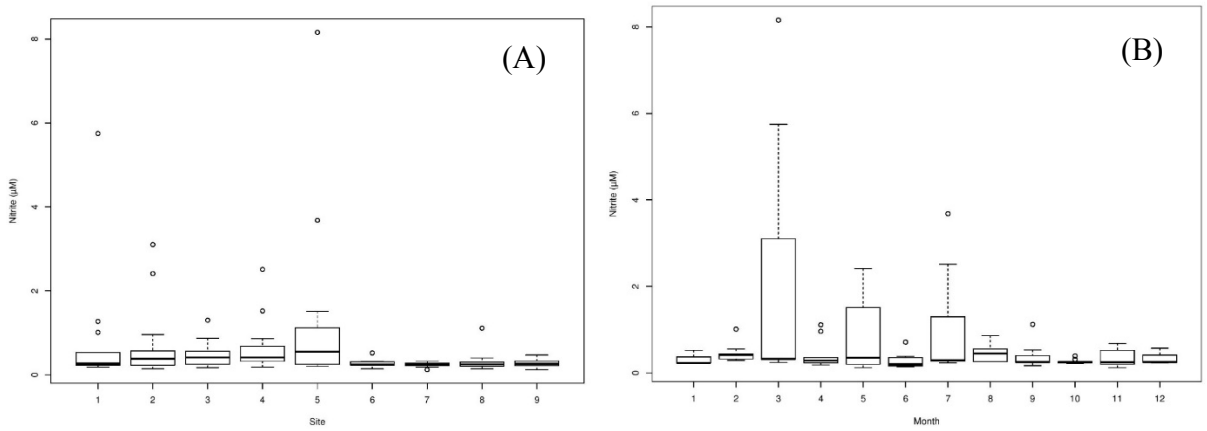

Figure B.1: Panel A shows box plot of NO_2^- concentrations by site and Panel B shows box plots of NO_2^- concentrations by month.

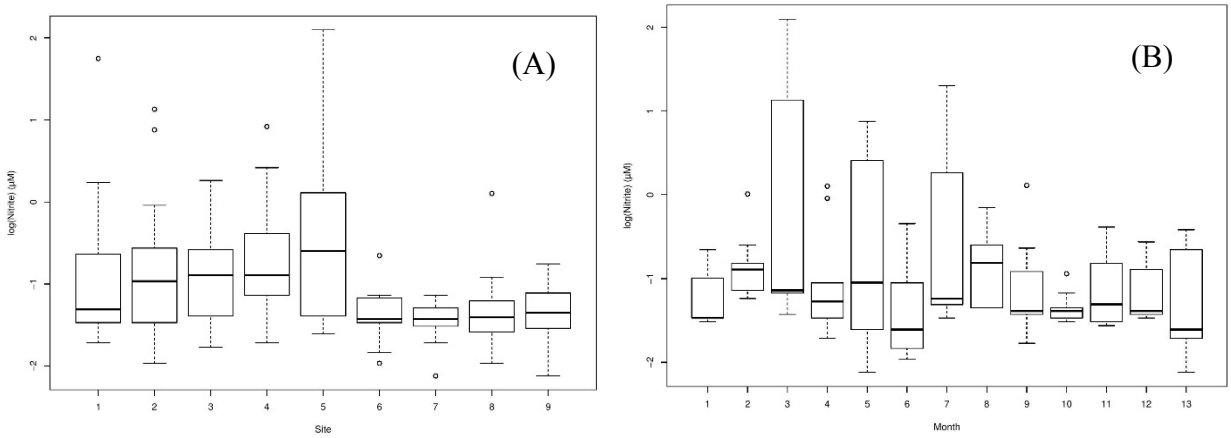

Figure B.2: Panel A shows box plot of log(NO_2^-) concentrations by site and Panel B shows box plots of log(NO_2^-) concentrations by month.

Appendix C

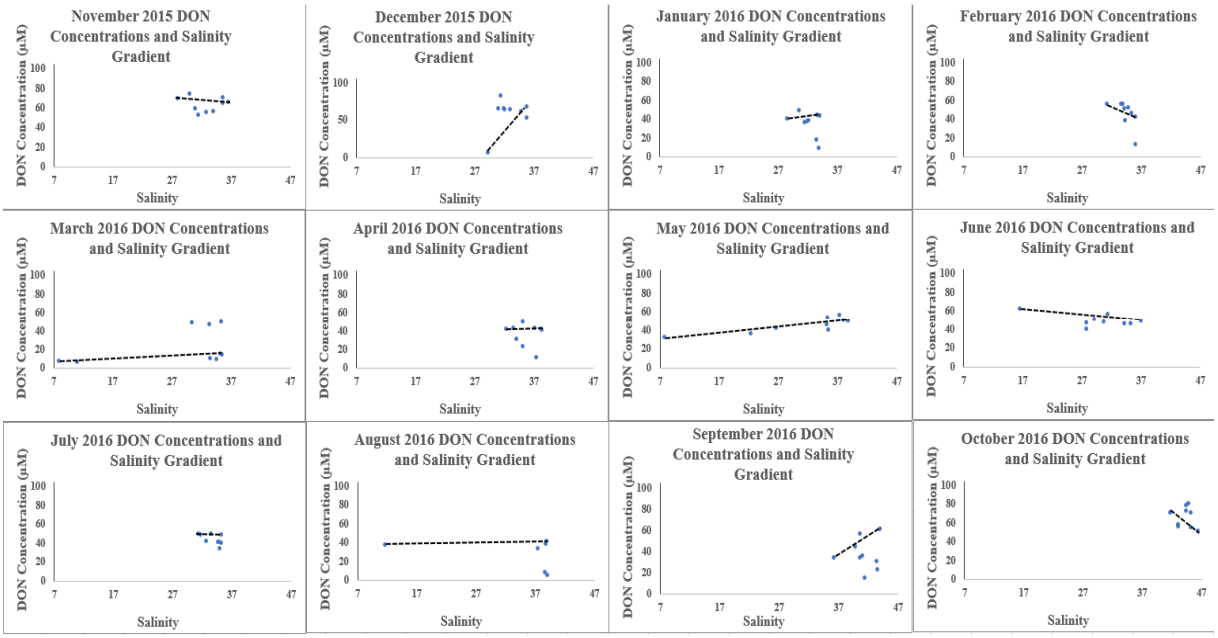

Figure C.1: Time series panel of DON plotted as a function of salinity. The line is drawn from the least to greatest salinity data points.

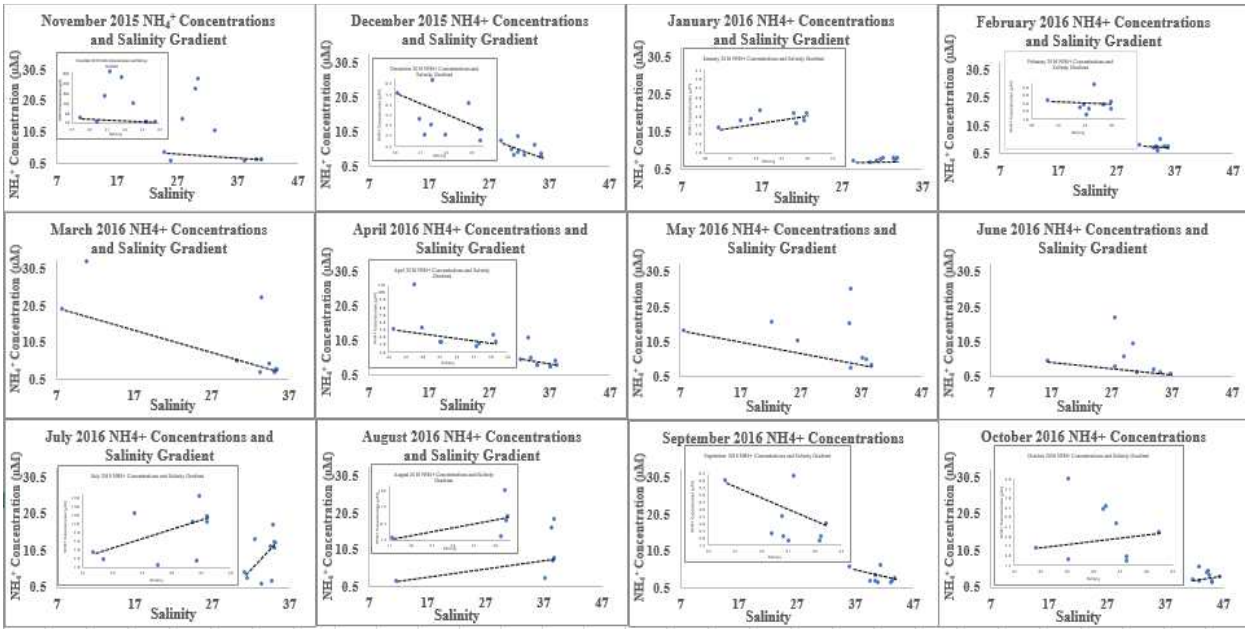

Figure C.2: Time series panel of NH_4^+ plotted as a function of salinity. The line is drawn from the least to greatest salinity data points.

Appendix D

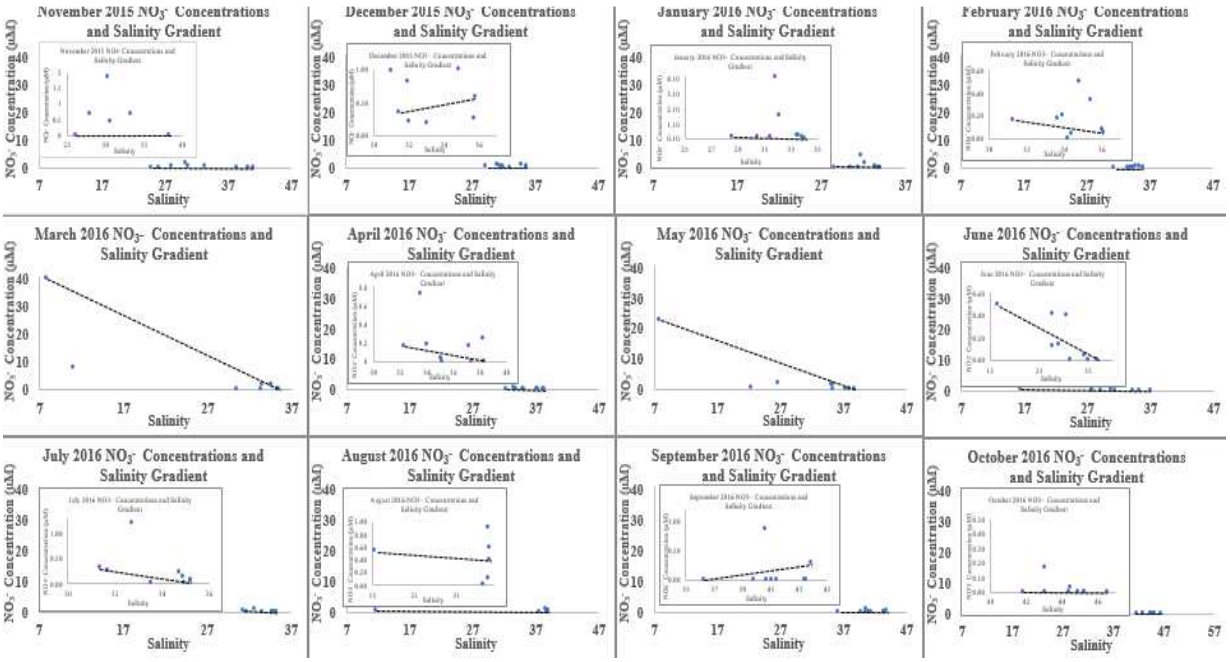

Figure D.1: Time series panel of NO_3^- plotted as a function of salinity. The line is drawn from the least to greatest salinity data points.

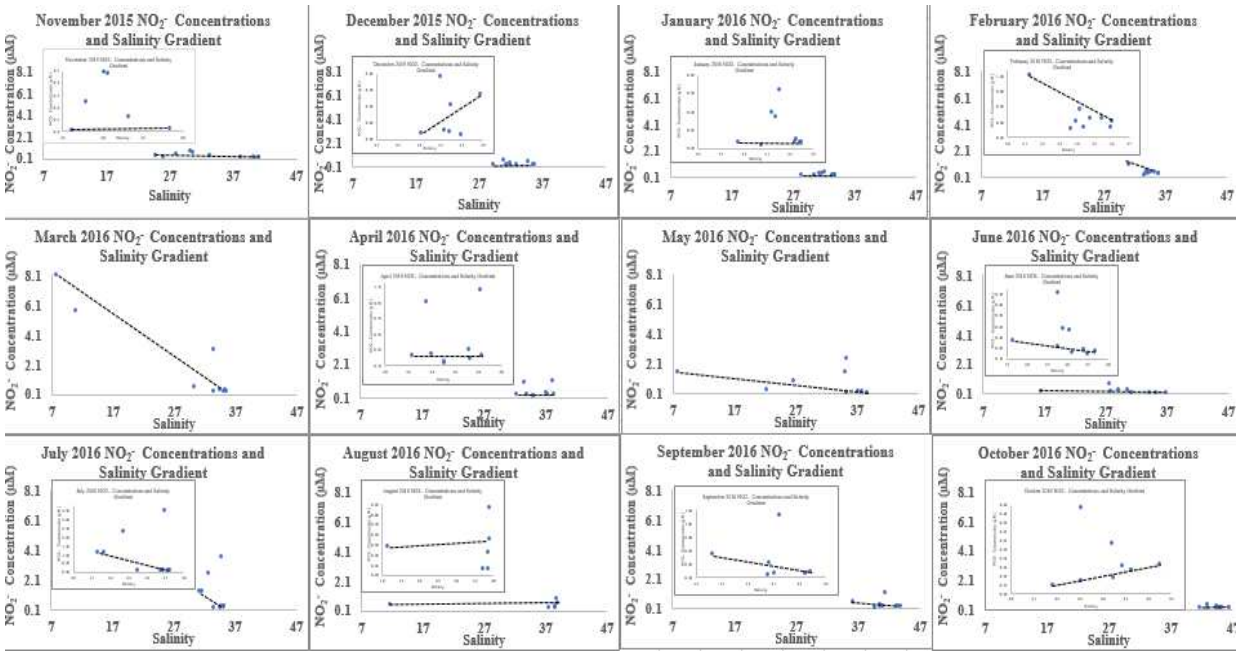

Figure D.2: Time series panel of NO_2^- plotted as a function of salinity. The line is drawn from the least to greatest salinity data points.

Appendix E

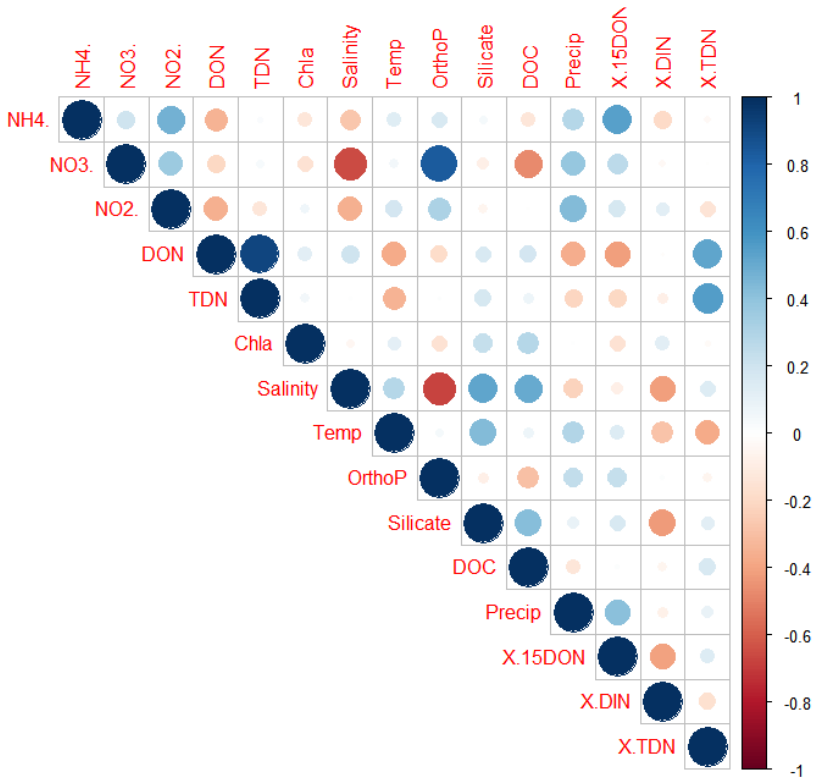

Figure E.1: Circle graphical representation of correlation plot of explanatory and dependent variables describing positive and negative relationships. The bigger the circle the more significant the correlation.

Appendix F

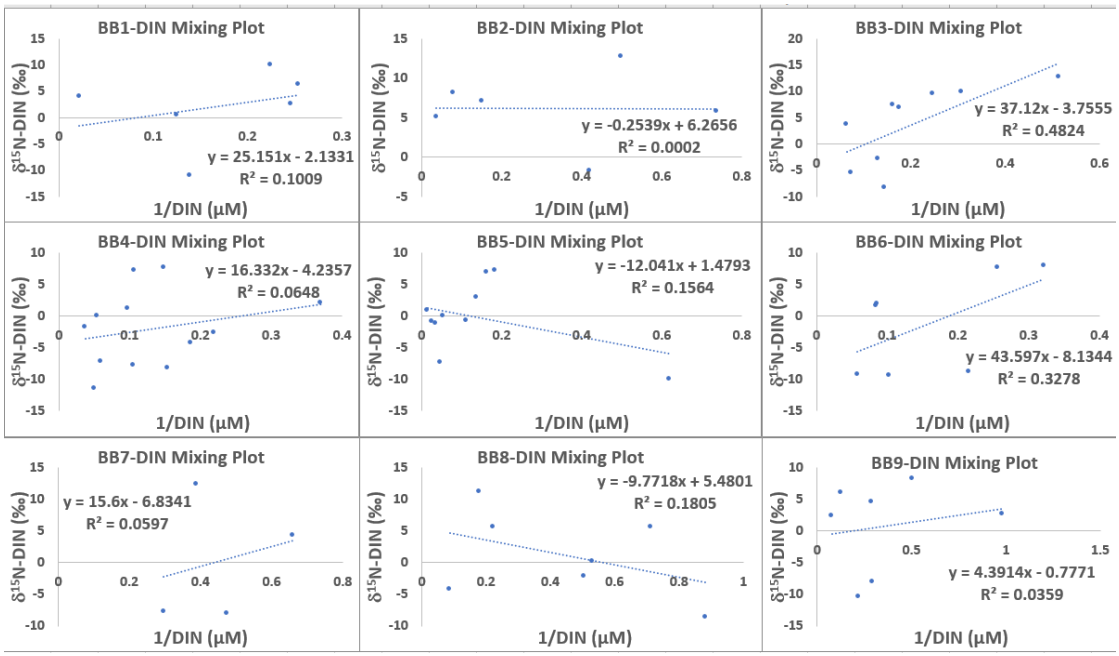

Figure F.1: Annual time series panel for each Baffin Bay Site of mixing plots for δ^{15}N-DIN values. δ^{15}N-DIN values are plotted as a function of 1/DIN concentration showing if δ^{15}N-DIN values exhibit linear mixing patterns or behave non-conservatively.

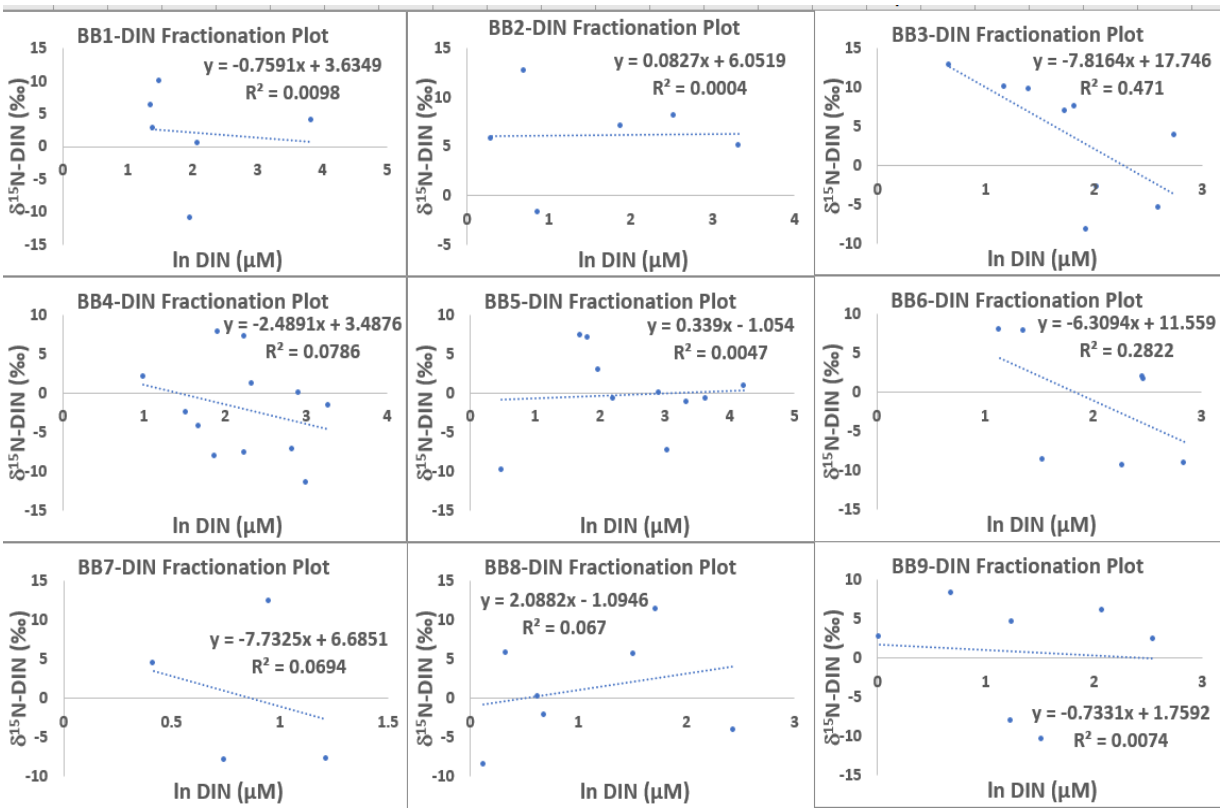

Figure F.2: Annual time series panel for each Baffin Bay Site of mixing plots for δ^{15}N-DIN values. δ^{15}N-DIN values are plotted as a function of ln (DIN) concentration showing if δ^{15}N-DIN values exhibit linear fractionation patterns or behave non-conservatively.

Appendix G

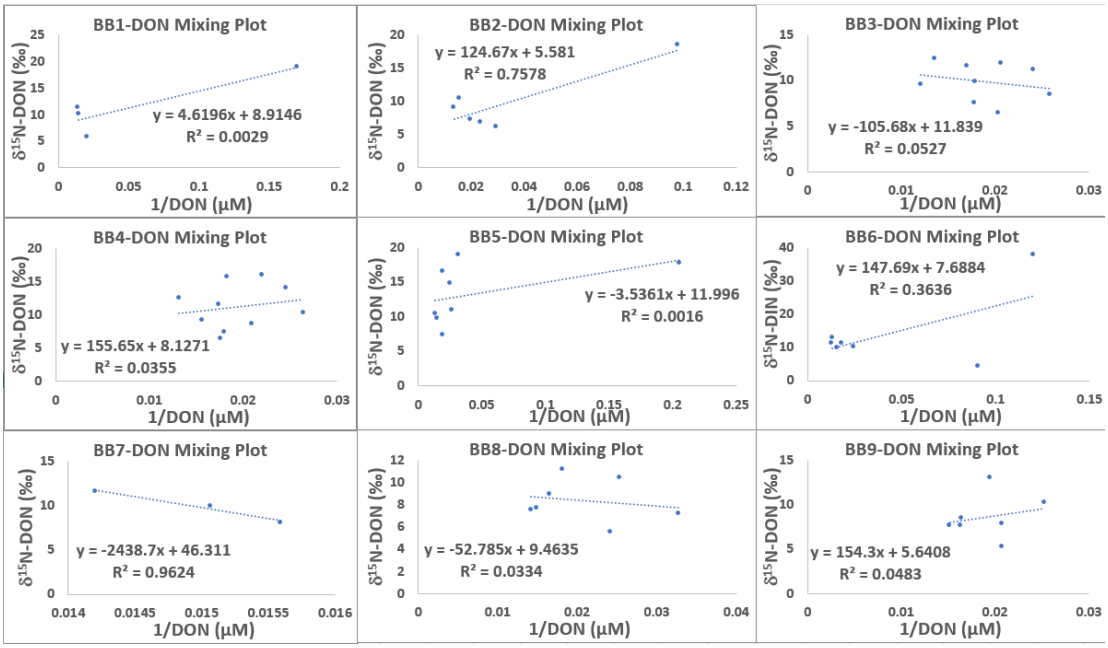

Appendix G.1: Annual time series panel for each Baffin Bay Site of mixing plots for δ^{15}N-DON values. δ^{15}N-DON values are plotted as a function of 1/DON concentration showing if δ^{15}N-DON values exhibit linear mixing patterns or behave non-conservatively.

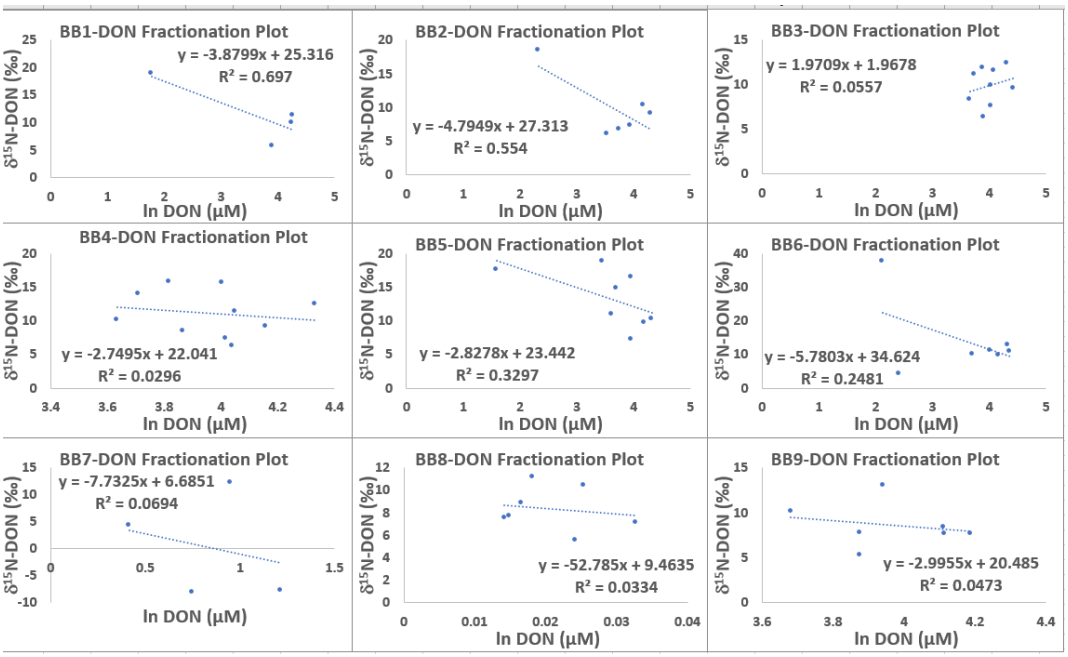

Appendix G.2: Annual time series panel for each Baffin Bay Site of mixing plots for δ^{15}N-DIN values. δ^{15}N-DIN values are plotted as a function of ln (DIN) concentration showing if δ^{15}N-DIN values exhibit linear fractionation patterns or behave non-conservatively.

Appendix H

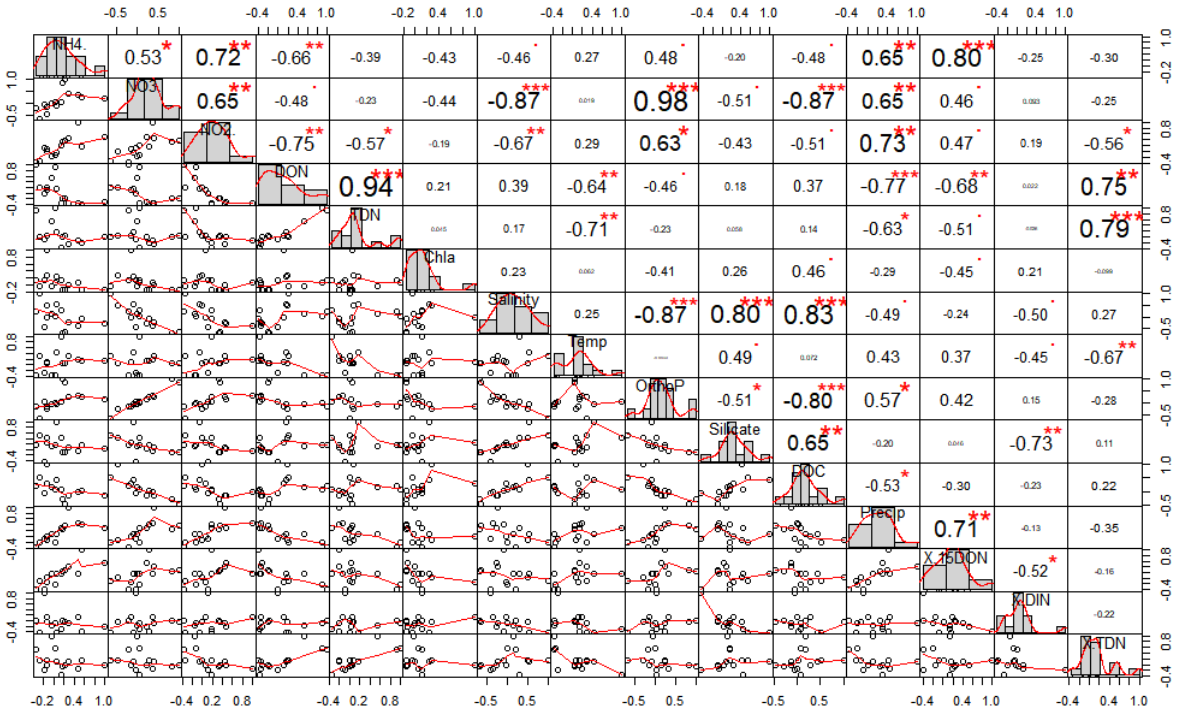

Figure H.1: Correlation plot of explanatory and dependent variables. Histograms in the diagonal show the distribution of the variable, the lower left hand of the graph shows a bivariate scatter plot with a fitted line, and the upper right hand of the plot shows the statistical significance of the correlation ((***): 0.001, (**):0.01, (*): 0.05.

Appendix I

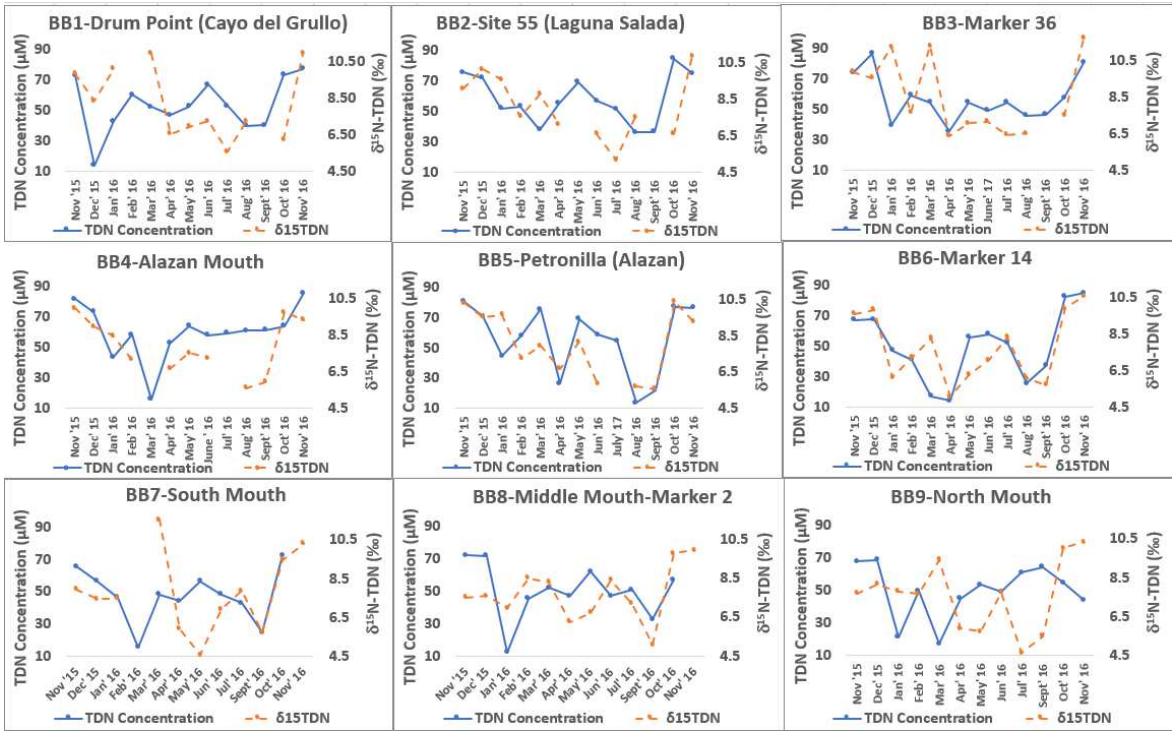

Appendix I.1: Time series panel of TDN concentration and corresponding δ^{15}N-TDN signatures over one year at each Baffin Bay sample site. The blue line corresponds to TDN concentrations and the orange line corresponds to δ^{15}N-TDN.

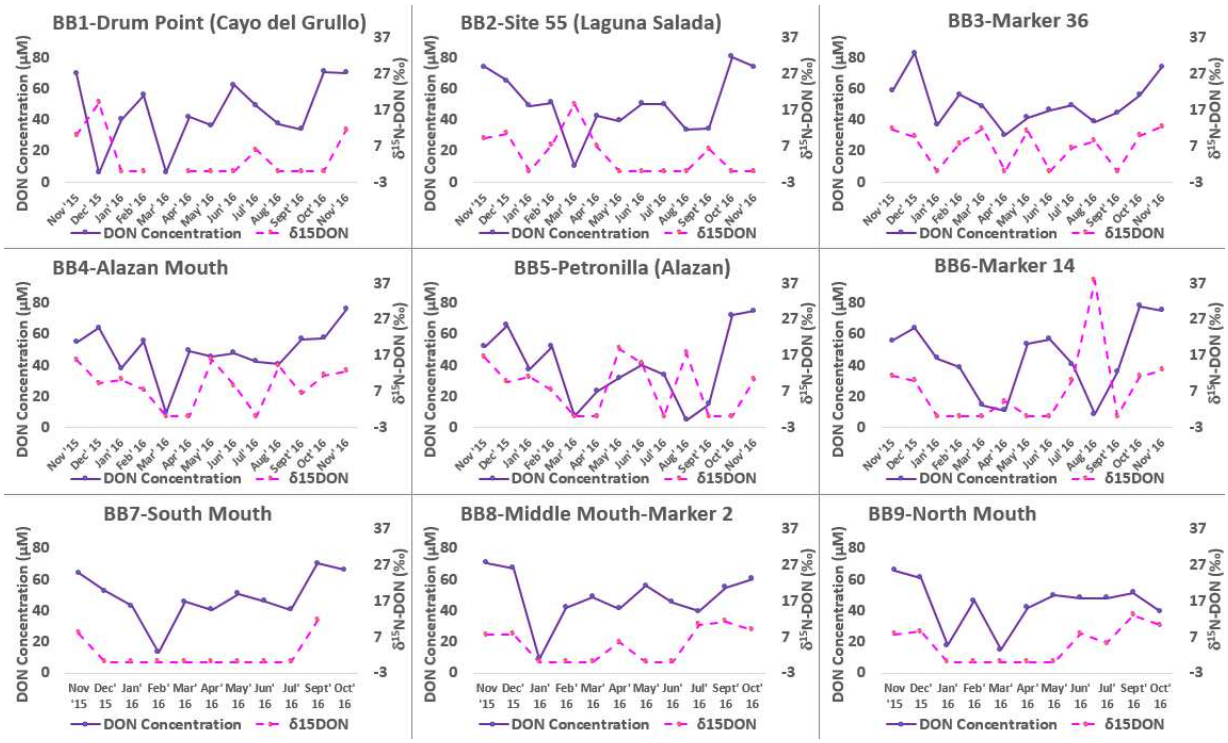

Appendix I.2: Time series panel of DON concentration and corresponding δ^{15}N-DON signatures over one year at each Baffin Bay sample site. The purple line corresponds to DON concentrations and the pink line corresponds to δ^{15}N-DON.

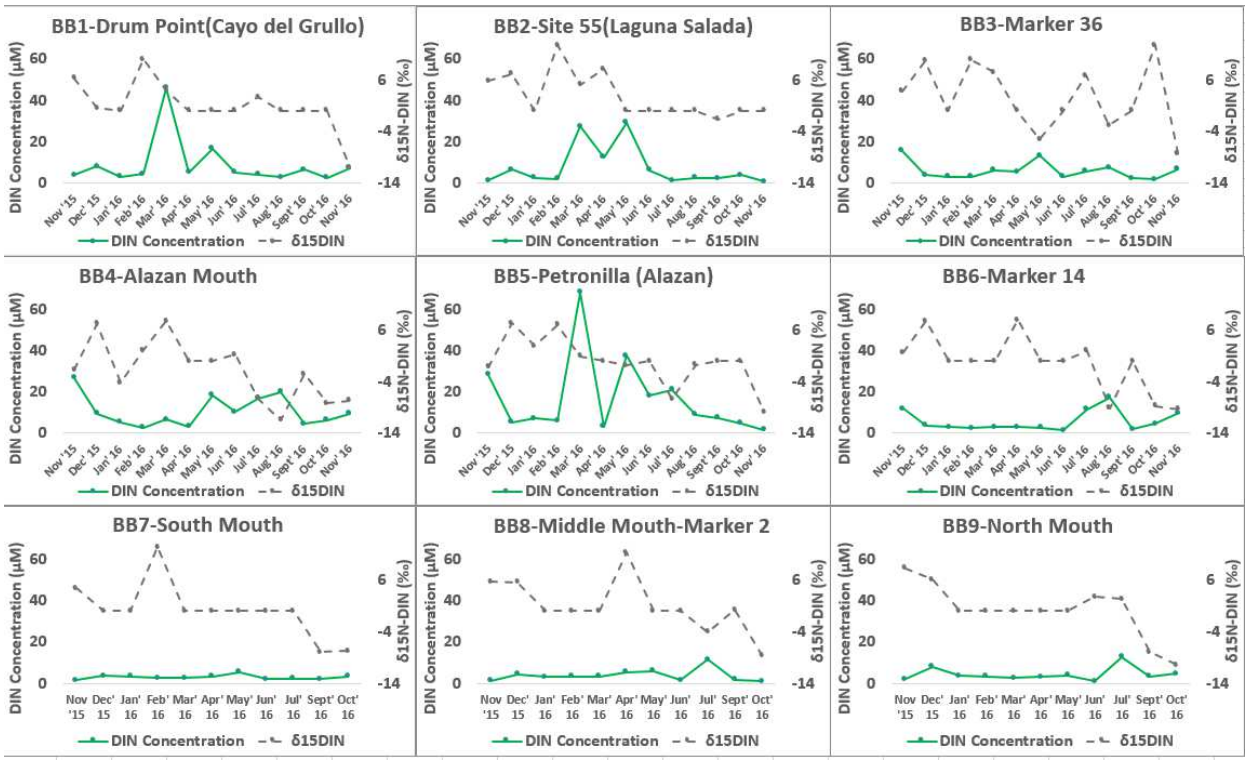

Appendix I.3: Time series panel of DIN concentration and corresponding δ^{15}N-DIN signatures over one year at each Baffin Bay sample site. The green line corresponds to DIN concentrations and the gray line corresponds to δ^{15}N-DIN.

Appendix J

Linear Model	Adjusted R Squared	F-statistic	p-value
39.69 -(0.31*Chlorophyll a) + (0.02*DOC μM) – (0.44*NH_4^+ μM) - (5.51*Orthophosphate) – (1.02*Precipitation) – (1.44*Salinity) + (0.52*temperature) – (0.33*δ^{15}N-DON)	0.5476	8.868	3.925e-07
50.81 - (0.44*Chlorophyll a) + (0.01*DOC μM) – (0.52*NH_4^+ μM) - (6.25*Orthophosphate) – (0.98*Precipitation) + (0.04*Silicate) – (1.76*Salinity) + (0.56*temperature) – (0.34*δ^{15}N-DON)	0.5615	8.40	4.271e-07

Table J.1: Table displaying formula for the top two linear models of the most significant explanatory variables for the dependent variable δ^{15}N-DIN including Adjusted R-squared, F-statistic, and p-value.

Linear Model	Adjusted R-Squared	F-statistic	p-value
6.93- (0.13*DON μM) + (0.27*NH_4^+ μM) - (0.20*δ^{15}N-DIN) + (1.08* δ^{15}N-TDN)	0.5179	15.5	2.599e-08
6.54 - (0.13*DON μM) + (0.26*NH_4^+ μM) - (0.20*δ^{15}N-DIN) + (1.06* δ^{15}N-TDN) + (0.78*Orthophosphate)	0.523	12.84	5.405e-08
1.74 + (0.01*DOC) - (0.14*DON μM) + (0.34*NH_4^+ μM) - (0.16*δ^{15}N-DIN) + (0.94* δ^{15}N-TDN) - (2.32*NO_2^- μM) +(0.41* NO_3^- μM)	0.5492	10.4	8.393e-08

Table J.2: Table displaying formula for the top three linear models of the most significant explanatory variables for the dependent variable δ^{15}N-DON including Adjusted R-squared, F-statistic, and p-value.

Linear Model	Adjusted R Squared	F-statistic	p-value
6.9+ (0.06*DON μM) + (0.06*NH_4^+ μM) + (0.14*NO_3^- μM) - (0.16*precipitation)	0.5766	23.81	5.027e-12
3.87+ (0.06*DON μM) + (0.07*NH_4^+ μM) + (0.18*NO_3^- μM) - (0.14*precipitation) + (0.04*salinity)	0.5833	19.76	1.008e-11
4.94+ (0.06*DON μM) + (0.06*NH_4^+ μM) + (0.14*NO_3^- μM) - (0.16*precipitation) + (0.003*silicate)	0.5773	19.3	1.552e-11

Table J.3: Table displaying formula for the top three linear models of the most significant explanatory variables for the dependent variable δ^{15}N-TDN including Adjusted R-squared, F-statistic, and p-value.

Appendix K

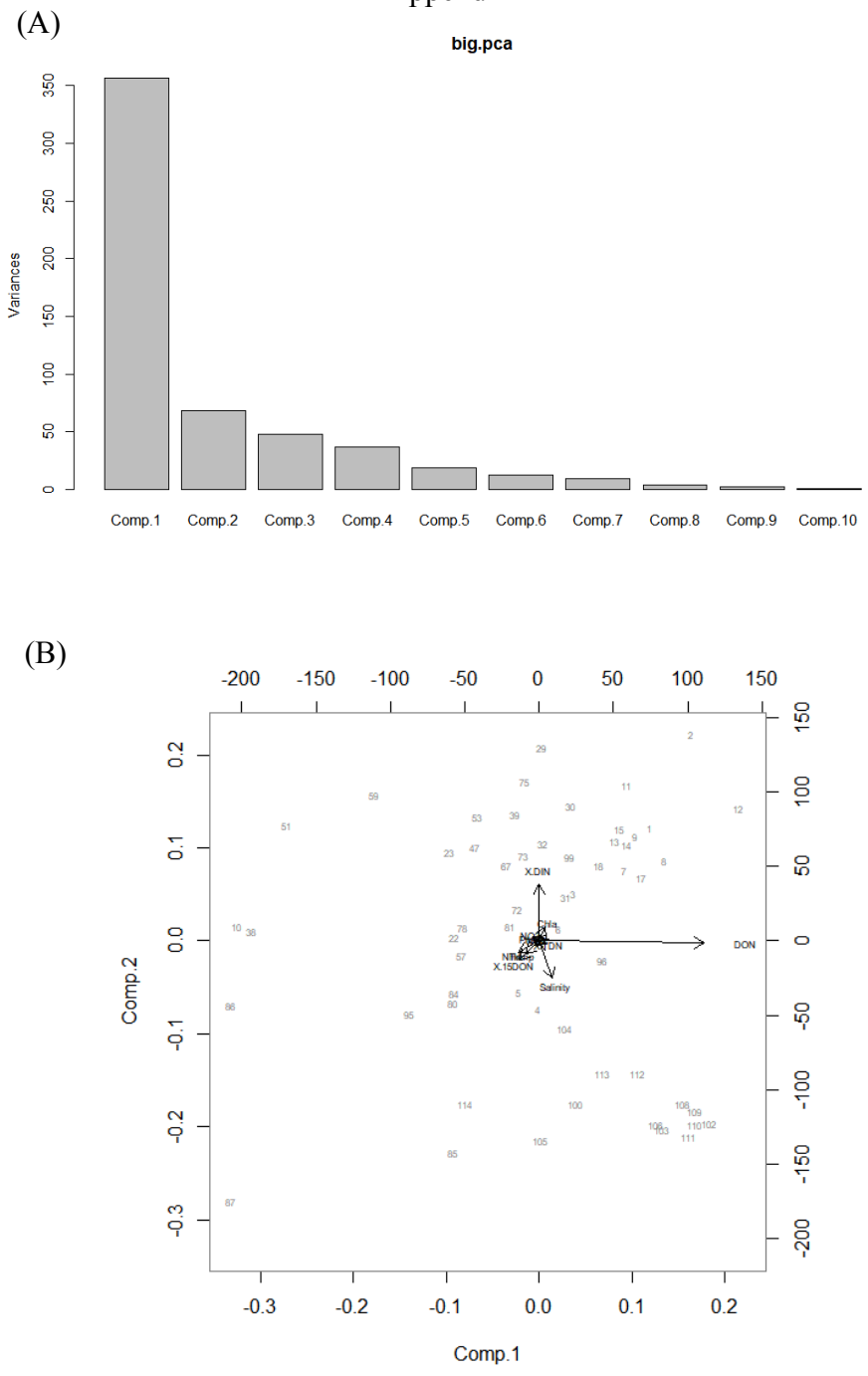

Figure K.1: Panel A: Bar graph of PCA component loadings showing Component 1 as the main contributer to the variability observed in the dataset. Panel B: Biplot of PCA results showing δ^{15}N-DIN and DON concentrations are the main contributors to Component 1.

Appendix L

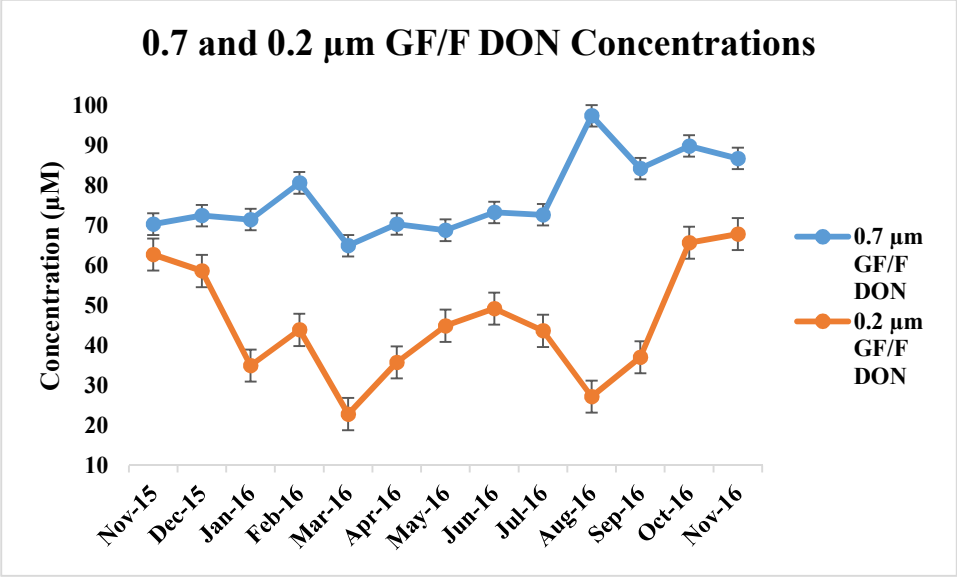

Figure L.1: Plot of site averages for DON concentrations filtered through both 0.2 µm and 0.7 µm GF/F over the study period.